


Differential Regulation of Prelimbic and Thalamic Transmission to the Basolateral Amygdala by Acetylcholine Receptors

Sarah C. Tryon, Joshua X. Bratsch-Prince, James W. Warren, Grace C. Jones, Alexander J. McDonald, and  David D. Mott

Department of Pharmacology, Physiology & Neuroscience, University of South Carolina School of Medicine, Columbia, South Carolina 29208

The amygdalar anterior basolateral nucleus (BLA) plays a vital role in emotional behaviors. This region receives dense cholinergic projections from basal forebrain which are critical in regulating neuronal activity in BLA. Cholinergic signaling in BLA has also been shown to modulate afferent glutamatergic inputs to this region. However, these studies, which have used cholinergic agonists or prolonged optogenetic stimulation of cholinergic fibers, may not reflect the effect of physiological acetylcholine release in the BLA. To better understand these effects of acetylcholine, we have used electrophysiology and optogenetics in male and female mouse brain slices to examine cholinergic regulation of afferent BLA input from cortex and midline thalamic nuclei. Phasic ACh release evoked by single pulse stimulation of cholinergic terminals had a biphasic effect on transmission at cortical input, producing rapid nicotinic receptor-mediated facilitation followed by slower mAChR-mediated depression. In contrast, at this same input, sustained ACh elevation through application of the cholinesterase inhibitor physostigmine suppressed glutamatergic transmission through mAChRs only. This suppression was not observed at midline thalamic nuclei inputs to BLA. In agreement with this pathway specificity, the mAChR agonist, muscarine more potently suppressed transmission at inputs from prefrontal cortex than thalamus. Muscarinic inhibition at prefrontal cortex input required presynaptic M4 mAChRs, while at thalamic input it depended on M3 mAChR-mediated stimulation of retrograde endocannabinoid signaling. Muscarinic inhibition at both pathways was frequency-dependent, allowing only high-frequency activity to pass. These findings demonstrate complex cholinergic regulation of afferent input to BLA that is pathway-specific and frequency-dependent.

Key words: amygdala; cholinergic; muscarinic; nicotinic; prefrontal; thalamus

Significance Statement

Cholinergic modulation of the basolateral amygdala regulates formation of emotional memories, but the underlying mechanisms are not well understood. Here, we show, using mouse brain slices, that ACh differentially regulates afferent transmission to the BLA from cortex and midline thalamic nuclei. Fast, phasic ACh release from a single optical stimulation biphasically regulates glutamatergic transmission at cortical inputs through nicotinic and muscarinic receptors, suggesting that cholinergic neuromodulation can serve precise, computational roles in the BLA. In contrast, sustained ACh elevation regulates cortical input through muscarinic receptors only. This muscarinic regulation is pathway-specific with cortical input inhibited more strongly than midline thalamic nuclei input. Specific targeting of these cholinergic receptors may thus provide a therapeutic strategy to bias amygdalar processing and regulate emotional memory.

Received Dec. 28, 2021; revised Dec. 12, 2022; accepted Dec. 14, 2022.

Author contributions: S.C.T., J.X.B.-P., A.J.M., and D.D.M. designed research; S.C.T., J.X.B.-P., J.W.W., and G.C.J. performed research; S.C.T., J.X.B.-P., and D.D.M. analyzed data; S.C.T. wrote the first draft of the paper; S.C.T., J.X.B.-P., A.J.M., and D.D.M. edited the paper; S.C.T. and D.D.M. wrote the paper.

This work was supported by National Institute of Mental Health R01MH104638 to D.D.M. and A.J.M.; University of South Carolina VP for Research ASPIRE2 Award to D.D.M.; University of South Carolina VP for Research Support to Promote the Advancement of Research and Creativity (SPARC) Research Grant; National Institutes of Health-NIGMS Grant T32-GM081740 to S.C.T.; and supported in part by Merit Award I01 BX001374 to Marlene A. Wilson (Principal Investigator) from the U.S. Department of Veterans Affairs Biomedical Laboratory Research and Development Service.

The authors declare no competing financial interests.

Correspondence should be addressed to David D. Mott at david.mott@uscmed.sc.edu.

<https://doi.org/10.1523/JNEUROSCI.2545-21.2022>

Copyright © 2023 the authors

Introduction

The basolateral amygdala is a brain region central to emotional processing and is necessary for associating cues with both positive and negative valence outcomes (LeDoux et al., 1990; Baxter and Murray, 2002; Janak and Tye, 2015). Compared with other brain regions, the basolateral amygdala, especially the anterior subdivision of the basolateral nucleus (BLA), receives the densest cholinergic projections from basal forebrain (BF) (Woolf, 1991; Muller et al., 2011; Zaborszky et al., 2012), suggesting that acetylcholine (ACh) plays a central role in regulating neurons in this region. Indeed, cholinergic mechanisms in the BLA are important

modulators of emotional memory (Power et al., 2003; McGaugh, 2004; Jiang et al., 2016; Wilson and Fadel, 2017). Cholinergic mechanisms in the BLA are also thought to regulate reward devaluation learning (Salinas et al., 1997), performance in tests of anxiety and depression-like behaviors (Mineur et al., 2016, 2018), and conditioned cue reinstatement of cocaine seeking (See et al., 2003; See, 2005), suggesting roles for ACh in the BLA in anxiety and fear disorders and drug addiction. These findings underscore the impact of cholinergic activity in the BLA in the pathophysiology of several neuropsychiatric diseases and highlight the need to better understand cholinergic modulation of the BLA.

ACh is thought to modulate neuronal circuits through both a slow mode of volume transmission as well as a more temporally precise phasic mode and thereby regulate neural activity over a range of temporal and spatial scales (Disney and Higley, 2020; Sarter and Lustig, 2020). These two modes of cholinergic transmission likely engage different types of ACh receptors with different kinetics, affinities, desensitization characteristics, and cellular locations. Thus, the nature of the cholinergic response may depend on the dynamics of ACh release. In the BLA, cholinergic signaling shapes neural activity through multiple mechanisms, including the regulation of presynaptic release probability (Jiang and Role, 2008; Jiang et al., 2016). Cholinergic projections from the BF converge with excitatory terminals providing an anatomic basis for cholinergic regulation of glutamatergic transmission in this area (Muller et al., 2011, 2013). As in other brain regions, ACh in the BLA is thought to act on presynaptic nicotinic receptors to enhance glutamate release (Jiang and Role, 2008; Jiang et al., 2016) and on muscarinic receptors to suppress release (Sugita et al., 1991; Yajeya et al., 2000). However, prior studies examining cholinergic modulation have used exogenous agonists or sustained optogenetic stimulation of cholinergic afferents, which results in broad spatial and temporal activation of cholinergic receptors. Evidence that cholinergic regulation can occur in a rapid and precise timescale sufficient to modulate individual synaptic events is lacking. This is significant as cholinergic neurons in BF can exhibit fast and precise responses to behaviorally relevant cues (Hangya et al., 2015; Crouse et al., 2020). Furthermore, little is known about the types of cholinergic receptors engaged by different modes of release or the relative role of ACh in modulating different afferent inputs to this region.

In the present study, we have investigated cholinergic regulation of afferent input to the BLA in mouse brain slices. The BLA receives major excitatory projections from prelimbic cortex (PL) and midline thalamic nuclei (MTN), which are thought to play distinct roles in amygdalar-dependent behaviors (Corcoran and Quirk, 2007; Arruda-Carvalho and Clem, 2014; Salay et al., 2018; Amir et al., 2019; Ahmed et al., 2021). We find that endogenously released ACh from single pulse optical stimulation can rapidly and precisely regulate glutamatergic transmission at cortical inputs, suggesting that cholinergic neuromodulation can serve precise, computational roles in the BLA at this timescale. This modulation differs from that during a sustained elevation of ACh, indicating involvement of different ACh receptors. During sustained ACh, cholinergic regulation is pathway-specific, producing stronger regulation of cortical than thalamic input. It is also frequency-dependent and acts as a high pass filter for incoming signals. Through these mechanisms, ACh dynamically shapes afferent input to BLA to bias amygdalar processing of salient cues.

Materials and Methods

Animals

All experiments were performed in adult *ChAT-Cre* mice (*B6;129S6-Chat^{tm2(cre)Low/J}*; JAX stock #006410) of either sex. These mice express Cre-recombinase under the control of the choline acetyltransferase gene. Alternately, in some experiments, the adult F1 progeny of *ChAT-Cre* mice crossed with *Ai32* mice (*B6;129S-Gt(Rosa)26SOR^{tm21(CAG-COP4⁺H134R/EYFP}Hze/J*, JAX stock #012569) were used. Mice were group-housed in a climate-controlled facility with a 12/12 light/dark cycle and provided with *ad libitum* access to food and water. All animal care and use procedures were approved by the University of South Carolina's Institutional Animal Care and Use Committee and performed in compliance with the guidelines approved by the National Institutes of Health's *Guide for the care and use of laboratory animals* (Department of Health and Human Services).

AAV delivery

Mice 1.5–3 months old were anesthetized under deep isoflurane anesthesia and placed in a stereotaxic surgery device (Stoelting). For *ex vivo* slice electrophysiology experiments using released ACh, 0.2 μ l of rAAV5-EF1a-DIO-hChR2(H134R)-EYFP (UNC Viral Vector Core) was delivered bilaterally into the BF, including the ventral pallidum/substantia innominata (from bregma: AP 1.2 mm; ML \pm 1.3 mm; DV -5.3 mm), the main source of cholinergic inputs to the BLA. For *ex vivo* slice electrophysiology experiments examining PL input to the BLA, 0.15 μ l of rAAV5-CAMKII-hChR2(H134R)-EYFP-WPRE (UNC Viral Vector Core) was delivered bilaterally to the PL (from bregma: AP 1.9 mm; ML \pm 0.3 mm; DV -2.0 mm). For experiments examining MTN input to the BLA, single injections of 0.2 μ l of rAAV5-CAMKII-hChR2(H134R)-EYFP-WPRE (UNC Viral Vector Core) were delivered to the MTN (from bregma: AP -0.3 mm; ML 0.0 mm; DV -3.9 mm). For experiments examining ventral subicular (vSUB) input to the BLA, single injections of 0.2 μ l of rAAV5-CAMKII-hChR2(H134R)-EYFP-WPRE (UNC Viral Vector Core) were delivered to the vSUB (from bregma: AP -2.5 mm; ML \pm 3.2 mm; DV -5.3 mm). Mice were used for experiments at least 3 weeks after surgery.

Immunofluorescence

To validate expression of channelrhodopsin in BF cholinergic neurons, *ChAT-Cre* mice injected in the BF with rAAV5-EF1a-DIO-hChR2(H134R)-EYFP or *ChAT-Cre/Ai32* mice were transcardially perfused with ice-cold PBS containing 0.5% nitrite followed with 4% PFA. Brains were postfixed overnight in 4% PFA at 4°C; 50 μ m coronal brain sections were cut using a vibratome (VT1200S, Leica). Slices were blocked in TBS containing 0.5% Triton X-100 and 10% normal donkey serum and incubated for 30 min at room temperature. Sections were then incubated for 48 h at room temperature in goat anti-ChAT primary antibody (1:1000, AB144P, Millipore). Following rinse, sections were again incubated at room temperature for 3 h in TBS containing an AlexaFluor-546-conjugated donkey anti-goat IgG secondary antibody (1:400, A-11056, Fisher Scientific), 0.5% Triton X-100, and 2% normal donkey serum. Sections were rinsed and mounted on slides with ProLong diamond antifade mountant DAPI (Fisher Scientific, P36971) and imaged on a Leica SP8 Multiphoton confocal microscope (Leica Microsystems). ChR2-EYFP was assessed by the endogenous EYFP fluorescent signal. The number of neurons positive for both EYFP and ChAT, or EYFP alone, were counted in each image using ImageJ (National Institutes of Health).

Slice preparation

Mice were deeply anesthetized with isoflurane and the brain quickly extracted and submerged in ice-cold (4°C) "cutting" ACSF containing the following (in mM): 110 choline chloride, 2.5 KCl, 25 NaHCO₃, 1.0 NaH₂PO₄, 20 glucose, 5 MgCl₂, 0.5 CaCl₂, and continuously bubbled with 95% O₂/5% CO₂. Choline chloride-based cutting solution with choline as a sodium-ion replacement has been previously used for slice electrophysiological recordings, as it preserves health of the slices (Hoffman and Johnston, 1998; Suzuki and Momiya, 2002).

Table 1. Drugs used in these experiments^a

Reagent	Target	Concentration	Source	Catalog #
4-DAMP	M3 receptors	1 μ M	Abcam	ab120144
AF-DX 116	M2 receptors	1 μ M	Abcam	ab120152
AM251	CB1 receptors	1 μ M	HelloBio	HB2776
AM630	CB2 receptors	2 μ M	Cayman Chemical	10006974
Atropine	mAChRs	5 μ M	Abcam	ab145582
Baclofen	GABA _B receptors	10 μ M	Millipore Sigma	B5399
Bicuculline	GABA _A receptors	10 μ M	HelloBio	HB0896
CGP55845 hydrochloride	GABA _B receptors	2 μ M	HelloBio	HB0960
CNQX	AMPA/kainate receptors	25 μ M	HelloBio	HB0204
D-APV	NMDARs	50 μ M	HelloBio	HB0225
Mecamylamine hydrochloride	nAChRs	10 μ M	Millipore Sigma	M9020
MK801 maleate	NMDARs	10 μ M	HelloBio	HB0004
Muscarine chloride	mAChRs	0.03–30 μ M	Millipore Sigma	M6532
N-ethylmaleimide	Gi/o protein subunit	50 μ M	Millipore Sigma	E3876
Oxotremorine-M	mAChRs	0.3 μ M	Tocris Bioscience	1067
Physostigmine (eserine hemisulfate salt)	Acetylcholinesterase	0.3–10 μ M	Millipore Sigma	E8625
Picrotoxin	GABA _A receptors	10–100 μ M	HelloBio	HB0506
Telenzepine dihydrochloride hydrate	M1 receptors	100 nM	Millipore Sigma	T122
VU0255035	M1 receptors	5 μ M	Abcam	ab141424
VU0467154	M4 receptors	3 μ M	StressMarq Biosciences	SIH-184
WIN 55212-2 mesylate	CB1 receptors	5 μ M	Tocris Bioscience	1038

^aFor each drug, the target, concentration used, source, and catalog number are provided.

2021; Perumal and Sah, 2022). Brains were cut into 300- μ m-thick (for whole-cell experiments) or 500- μ m-thick (for field recordings) coronal sections using a vibratome (VT1000S, Leica). Slices were transferred to an incubation chamber filled with warmed ACSF containing the following (in mM): 125 NaCl, 2.7 KCl, 25 NaHCO₃, 1.25 NaH₂PO₄, 10 glucose, 5 MgCl₂, 0.5 CaCl₂, and bubbled with 95% O₂/5% CO₂ at 34°C–36°C. After a minimum of 20 min, the incubation temperature was allowed to equilibrate to room temperature for at least 40 min before slices were used for recording.

Slice electrophysiology recordings

For recording, slices were placed in a submersion chamber and continuously perfused with oxygenated (95% O₂/5% CO₂), recording ACSF at a rate of 4–6 ml/min (for field potentials) or 1–2 ml/min (for whole cell) at 30°C–32°C. Recording ACSF contained the following (in mM): 125 NaCl, 2.7 KCl, 25 NaHCO₃, 1.25 NaH₂PO₄, 10 glucose, 1 MgCl₂, 2 CaCl₂ (pH 7.4, 305 mOsm). Field potentials were recorded from the BLA with an Axoprobe 1A amplifier (Molecular Devices) using borosilicate glass electrodes, which had a resistance of 1–3 M Ω when filled with recording ACSF. For whole-cell recording, pyramidal neurons in the BLA were visualized using infrared-differential interference contrast optics through a 40 \times objective (Olympus BX51WI). Borosilicate glass electrodes of 4–6 M Ω resistance were used for recordings and filled with a potassium gluconate internal solution consisting of the following (in mM): 135 K-gluconate, 5 KCl, 10 HEPES, 2 MgCl₂, 2 MgATP, 0.3 NaGTP, and 0.5 EGTA. Voltage-clamp recordings were made at a holding potential of –70 mV with a Multiclamp 700B (Molecular Devices) amplifier. Experiments were discarded if significant changes occurred in input or series resistance which were monitored throughout. All responses were filtered at 1 kHz, digitized using a Digidata 1440A A-D board (Molecular Devices) and analyzed using pClamp10 software (Molecular Devices).

To evoke glutamatergic field EPSPs (fEPSPs), PL or MTN fibers expressing hChR2(H134R)-EYFP were stimulated with single or dual (50 ms apart) pulses (1–3 ms duration) of 490 nm blue LED light (M490F3, ThorLabs) delivered through a fiber optic cable directly over the recording site in the BLA every 30 s. For whole-cell recording, the pulse of 490 nm blue light (pE-4000, CoolLED) was delivered through the 40 \times objective. Alternately, in some experiments, fEPSPs or whole-cell EPSCs in BLA were electrically evoked using a 0.1 ms current pulse delivered through a monopolar platinum-iridium stimulating electrode (FHC) placed in the external capsule (EC). A two-opsin strategy to independently activate PL and MTN inputs was not used

due, in part, to concerns about cross-talk between the opsins under the conditions of our field potential experiments (Venkatachalam and Cohen, 2014; Christoffel et al., 2021). Non-NMDA glutamatergic responses were pharmacologically isolated by blocking GABA_A receptors (10–100 μ M picrotoxin or 10 μ M bicuculline), GABA_B receptors (2 μ M CGP55845), and NMDA receptors (50 μ M D-APV or 10 μ M MK801). CNQX (25 μ M) was added at the conclusion of some experiments to confirm that the response was mediated by AMPA/kainate receptors.

To study the effects of released ACh, cholinergic fibers expressing hChR2(H134R)-EYFP were optogenetically stimulated with 2–3 ms pulses of 490 nm blue LED light delivered directly over the recording site in the BLA every 90 s. A single light pulse was delivered either immediately (2 ms) before or 250 ms before electrical stimulation. Alternately, a theta burst of light [4 bursts of light (four pulses at 50 Hz) every 200 ms] was delivered 250 ms before electrical stimulation (such that the last light pulse in the burst was 250 ms before electrical stimulation). In whole-cell experiments to determine the effect of light on the EPSC amplitude, any direct postsynaptic currents produced by optically released ACh alone were recorded and subtracted from evoked EPSC traces where light was applied.

Drugs. Drugs used in this study are listed in Table 1. Baclofen, muscarine chloride, N-ethylmaleimide, mecamylamine, physostigmine, and telenzepine were purchased from Millipore Sigma. Bicuculline, D-APV, CNQX, CGP55845 hydrochloride, MK 801 maleate, picrotoxin, and AM251 were purchased from HelloBio. WIN 55212-2 and oxotremorine-M were purchased from Tocris Bioscience. 4DAMP, AF-DX 116, VU0255025, and atropine were purchased from Abcam. AM630 was purchased from Cayman Chemical, and VU0467154 was purchased from StressMarq Biosciences. All reagents were added from freshly prepared stock solution to the ACSF. Drugs were applied using bath perfusion and drug concentration in the bath during wash-in was allowed to equilibrate before measurements were taken.

Data analysis and statistics

Electrophysiological data analysis was performed using pClamp 10 (Molecular Devices) and OriginPro 2018b (Microcal) software. For released ACh experiments, consecutive sweeps in “Light ON” or “Light OFF” conditions (2–6 sweeps) were averaged and the peak amplitude of the averaged EPSC or fEPSP was measured. For experiments involving optogenetically stimulated PL and MTN input and bath application of muscarine, the peak amplitude of fEPSPs was measured as the average peak amplitude of the steady-state evoked

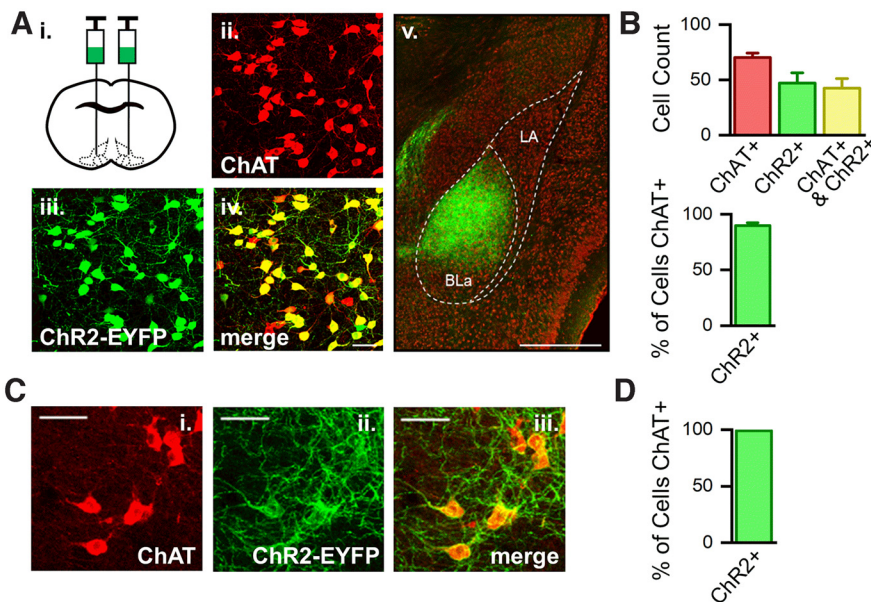


Figure 1. ChR2 expression in ChAT⁺ neurons. **A**, Viral injection into the BF of *ChAT-cre* mice led to ChR2-EYFP expression in ChAT-containing neurons that project to BLA. **Ai**, Schematic of injection sites. **Aii**, ChAT-immunopositive cell bodies (red) at the injection site. **Aiii**, EYFP-labeled ChR2⁺ cells (green) at the injection site. **Aiv**, Merged image showing that ChR2-EYFP cells are immunopositive for ChAT (yellow). Scale bar, 50 μ m. **Av**, In the same mouse, ChR2-EYFP-expressing axons (green) strongly innervate the BLA. Scale bar, 500 μ m. **B**, Top, Counts of BF neurons per 50- μ m-thick coronal tissue section that were labeled with ChAT⁺ (red), ChR2-EYFP⁺ (green), or both (yellow). Bottom, The majority of cells expressing ChR2-EYFP ($89.8 \pm 2.4\%$, $N = 5$) were also immunopositive for ChAT. **C**, ChAT-immunopositive cells (red) in BF of *ChAT-Cre/Ai32* mice. **Cii**, EYFP-labeled ChR2⁺ cells (green) in BF. **Ciii**, Merged image. Scale bar, 50 μ m. **D**, In *ChAT-Cre/Ai32* mice, the majority of neurons ($99.1 \pm 0.8\%$, $N = 3$) expressing ChR2-EYFP are also immunopositive for ChAT.

fEPSP response in each pharmacological condition. All peak amplitudes were normalized to the baseline condition (“control”) and are expressed as the mean \pm SEM. Concentration–response curves represent a least-squares fit of each dataset to a sigmoidal (logistic) curve (GraphPad Prism, GraphPad Software). The IC₅₀ and Hill slope were calculated from this curve. Means, SEs and 95% CIs were determined by the fitting algorithm. In some experiments, multiple slices per animal were used, so for all experiments, n = slice number and N = animal number. Statistical significance was determined using a Student’s *t* test (paired or unpaired), a one-way ANOVA, or a repeated-measures ANOVA with a *post hoc* Tukey test ($\alpha < 0.05$ was taken as significant).

Results

Immunofluorescent verification of ChR2 expression in BLA-projecting cholinergic neurons in the BF

In order to optogenetically evoke ACh release, two strategies were used to selectively express channelrhodopsin in BF cholinergic axons in BLA. First, ChR2-EYFP was expressed in BF cholinergic neurons of *ChAT-Cre* mice through Cre-dependent rAAV-mediated transfection (Unal et al., 2015; Aitta-aho et al., 2018). Four weeks after AAV injection, we verified selective ChR2-EYFP expression in neurons labeled with ChAT antibody (ChAT⁺) in the BF (Fig. 1*A,B*). Cell counts of ChAT⁺ neurons, ChR2-EYFP⁺ neurons (ChR2⁺), or neurons expressing both ChAT⁺ and ChR2-EYFP⁺ at the injection site revealed that most ChAT⁺ neurons expressed ChR2-EYFP ($70.2 \pm 4.26\%$, $N = 5$, Fig. 1*B*). Furthermore, immunoreactivity for ChAT in the majority of ChR2-EYFP⁺ cells ($89.8 \pm 2.4\%$, $N = 5$) confirmed that expression of ChR2 was restricted to cholinergic neurons in this region (Fig. 1*B*, bottom). Axons from labeled ChAT⁺ neurons in BF densely innervated the BLA (Fig. 1*Av*), as previously described (Aitta-aho et al., 2018), further supporting the selective labeling of cholinergic projections to BLA.

Channelrhodopsin was also expressed in ChAT⁺ neurons using a double transgenic strategy in which *ChAT-Cre* mice were crossed with an *Ai32* reporter mouse line expressing Cre-dependent ChR2-EYFP (Hedrick et al., 2016; Baker et al., 2018). In the F1 generation of these mice (*ChAT-Cre/Ai32* mice), the majority of BF ChAT⁺ neurons ($80 \pm 3\%$, 877 cells, $N = 3$) were immunopositive for ChR2-EYFP. Furthermore, immunoreactivity for ChAT in most ChR2-EYFP-immunopositive cells ($99.1 \pm 0.8\%$, 694 cells, $N = 3$) confirmed that expression of ChR2 was restricted to cholinergic neurons (Fig. 1*C,D*). Notably, the BLA of these mice did not contain any cell bodies positive for ChR2, ensuring selective activation of BF derived cholinergic terminals with optogenetic stimulation during BLA slice recordings.

Synaptically released ACh biphasically regulates cortico-amygdalar transmission in the BLA through both nicotinic and muscarinic receptors

In vivo recordings indicate that a behaviorally relevant cue can recruit BF cholinergic neurons to synchronously fire a single, precisely timed spike or brief burst of action potentials (Hangya et al., 2015). To determine the effect of this cholinergic

neuron activity on afferent input to the BLA, cholinergic terminals were stimulated with a single blue light pulse (490 nm) and the effect on synaptic transmission at cortical inputs to BLA in *ChAT-Cre/Ai32* mice examined. EPSCs were evoked in BLA pyramidal cells by electrical stimulation of cortical afferents in the EC (Fig. 2*A*) (Jiang et al., 2016). Optogenetic stimulation of cholinergic terminals had a biphasic effect on the amplitude of this EPSC in the majority of cells (Fig. 2). Stimulation of cholinergic terminals immediately (2 ms) before stimulation of cortical afferents (Early interval) evoked a facilitation of the EPSC. This early facilitation was sensitive to the frequency at which cholinergic terminals were stimulated. In these experiments, cholinergic terminals were stimulated every 90 s, as stimulation at shorter intervals resulted in a rundown or loss of the facilitation. The extent of the facilitation varied between cells (range: 92%–137%, mean: $107.5 \pm 2\%$, $n = 23$, $N = 10$) with 17 of 23 cells (73.9%) exhibiting a facilitation (Fig. 2*C*). Increasing the interval between the light pulse and cortical afferent stimulation caused this facilitation to rapidly diminish and become a depression at intervals > 20 ms. When the cortical afferents were stimulated 250 ms after the light pulse, the EPSC was suppressed (range: 46%–96%; mean: $79.4 \pm 3\%$; $n = 17$, $N = 10$; Fig. 2*C,D*) with 17 of 17 cells (100%) showing inhibition. All cells that exhibited early facilitation also exhibited late inhibition. However, EPSCs in five cells exhibited late inhibition with no early facilitation. Late inhibition was similar in amplitude whether cholinergic terminals were stimulated with a single light pulse or a theta burst [4 bursts of light (four pulses at 50 Hz) delivered every 200 ms] of light pulses (Fig. 2*D*).

Pharmacological analysis revealed that the early facilitation by ACh was completely blocked by the nicotinic antagonist, mecamylamine (10 μ M; Fig. 3*A*), indicating that it was nAChR-mediated. Mecamylamine had no effect on the EPSC amplitude at the

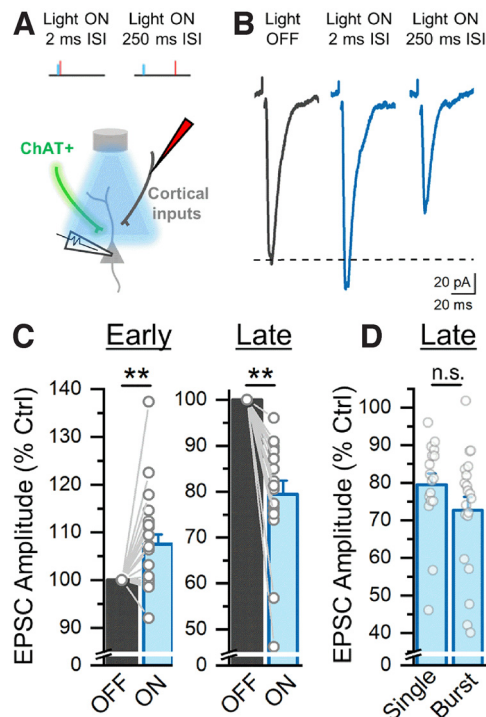


Figure 2. Released ACh exerts a biphasic effect on the cortical EPSC in BLA. **A**, Schematic illustrating the placement of a stimulating electrode in the EC and recording electrode in the BLA. Blue light pulses (490 nm, 1 ms) were delivered above the recording site to stimulate cholinergic terminals before EC stimulation. Top, “Light ON: Early” illustrates an EC stimulus delivered immediately (2 ms) after a single light pulse. “Light ON: Late” illustrates an EC stimulus delivered 250 ms after a single light pulse. **B**, **C**, Optogenetic activation of cholinergic terminals evoked facilitation of the EC-evoked EPSC at the early interval ($n = 23$, $N = 10$; paired t test, $p = 0.0013$) and inhibition at the late interval ($n = 17$, $N = 10$; paired t test, $p = 0.0045$). The extent of facilitation or inhibition varied between cells (open circles). Facilitation at the early interval was absent in 6 cells, while inhibition was present at the late interval in all cells. **D**, Inhibition at the late interval was similar (two-sample t test, $p = 0.17$) whether it was evoked by a single pulse (1 ms, $n = 17$) or burst of blue light pulses (4 bursts of light [4 pulses at 50 Hz] delivered every 200 ms, $n = 20$). $**p < 0.01$.

250 ms interval (Fig. 3C), demonstrating the absence of any delayed effect of nAChRs on the EPSC, as has been reported in cortex (Urban-Ciecko et al., 2018). The rundown of this nicotinic response at stimulus intervals <90 s is consistent with nAChR desensitization or depletion of transmitter in the presynaptic cholinergic terminal, as has been reported in hypothalamus (Hatton and Yang, 2002). However, other factors, such as presynaptic inhibition of ACh release, may also contribute (Zhang et al., 2002). The site of action of nAChRs was investigated by examining the effect of cholinergic stimulation on paired pulse facilitation. Nicotinic facilitation significantly reduced the paired pulse ratio at the early interval (Fig. 3B), indicating a presynaptic site of action in agreement with prior studies (Jiang and Role, 2008; Cheng and Yakel, 2014; Tang et al., 2015). In contrast, late cholinergic suppression of the EPSC was blocked by bath application of the muscarinic antagonist, atropine ($5 \mu\text{M}$; Fig. 3C), demonstrating that it was mAChR-mediated. This mAChR-mediated depression of the EPSC significantly increased the paired pulse ratio at the later interval (Fig. 3D), suggesting that the mAChRs were also presynaptic.

A similar cholinergic-induced late inhibition of cortical-evoked transmission was also evident in field potential recordings in the BLA. As shown in Figure 3E, EC stimulation evoked fEPSPs in BLA that reflected EPSCs in pyramidal neurons during

whole-cell recording. Optogenetic stimulation of cholinergic terminals with theta burst stimulation [4 bursts of light (four pulses at 50 Hz) delivered every 200 ms] significantly inhibited the fEPSP evoked by EC stimulation 250 ms later. Theta burst stimulation of cholinergic terminals was subsequently delivered every 90 s to study cholinergic inhibition of the cortical fEPSP. Theta burst stimulation was chosen for these studies to reflect BF activity during active waking and paradoxical sleep (Lee et al., 2005). Cholinergic inhibition of the fEPSP was unaffected by mecamylamine ($10 \mu\text{M}$) but was completely reversed by application of atropine ($5 \mu\text{M}$; Fig. 3F), indicating that it was muscarinic receptor-mediated. Together, these findings suggest that single pulse stimulation of ACh terminals evokes a biphasic modulation of cortical input by ACh, whereby ACh acts via a precisely timed action on presynaptic nAChRs to rapidly facilitate cortical neurotransmission to the BLA and on presynaptic mAChRs to cause a delayed suppression. Similarly, an mAChR-mediated delayed suppression of fEPSPs is also seen following theta pattern stimulation of ACh release.

ACh differentially regulates cortical and thalamic input to the BLA

A behaviorally salient cue can recruit BF cholinergic neurons to fire, producing a phasic release of ACh into BLA (Aitta-aho et al., 2018; Crouse et al., 2020). In contrast, during prolonged emotional arousal, extracellular ACh levels in the amygdala exhibit a sustained increase (Kellis et al., 2020). To investigate the impact of sustained ACh on synaptic transmission, we increased endogenous, extracellular ACh by applying physostigmine to inhibit acetylcholinesterase, the enzyme that catalyzes the breakdown of ACh. We compared the effect of increasing concentrations (0.3 – $10 \mu\text{M}$) of physostigmine on the amplitude of the EC-evoked fEPSP. Blocking AChE led to a concentration-dependent suppression of the EC-evoked fEPSP (Fig. 4A,B). Antagonism of muscarinic receptors ($5 \mu\text{M}$ atropine) reversed this suppression, indicating that the inhibition was muscarinic receptor-mediated. The ability of AChE inhibition alone to suppress the EC-evoked fEPSP in the absence of stimulation of cholinergic inputs demonstrates the presence of endogenously released ACh in the brain slice and suggests that the impact of released ACh on synaptic transmission in this pathway is limited by this enzyme, in line with previous studies (Aitta-aho et al., 2018).

Inputs from both cortex and MTN exert significant influence over BLA activity to regulate amygdalar responses to emotionally arousing stimuli (Corcoran and Quirk, 2007; Arruda-Carvalho and Clem, 2014; Salay et al., 2018; Amir et al., 2019; Ahmed et al., 2021). Cholinergic mechanisms have the potential to play a significant role in shaping afferent input through these pathways. However, the relative role of ACh in regulating transmission in these pathways has not been examined. To compare cholinergic regulation of thalamic and cortical inputs, we injected an rAAV containing ChR2-EYFP under the control of the CaMKII promoter into the MTN of mice. After at least 3 weeks, brain slices were prepared and glutamatergic terminals in BLA from MTN and cortex were stimulated in the same slice and evoked field responses recorded at the same site. MTN fEPSPs were evoked by optogenetic stimulation of MTN terminals in BLA with single pulses of blue light, while cortical fEPSPs were evoked by electrical stimulation of cortical afferents in the EC (Fig. 3E). The effect of a sustained increase in ACh was assessed in each pathway following application of physostigmine ($10 \mu\text{M}$). As previously observed (Fig. 4A), elevated ACh strongly suppressed the cortical

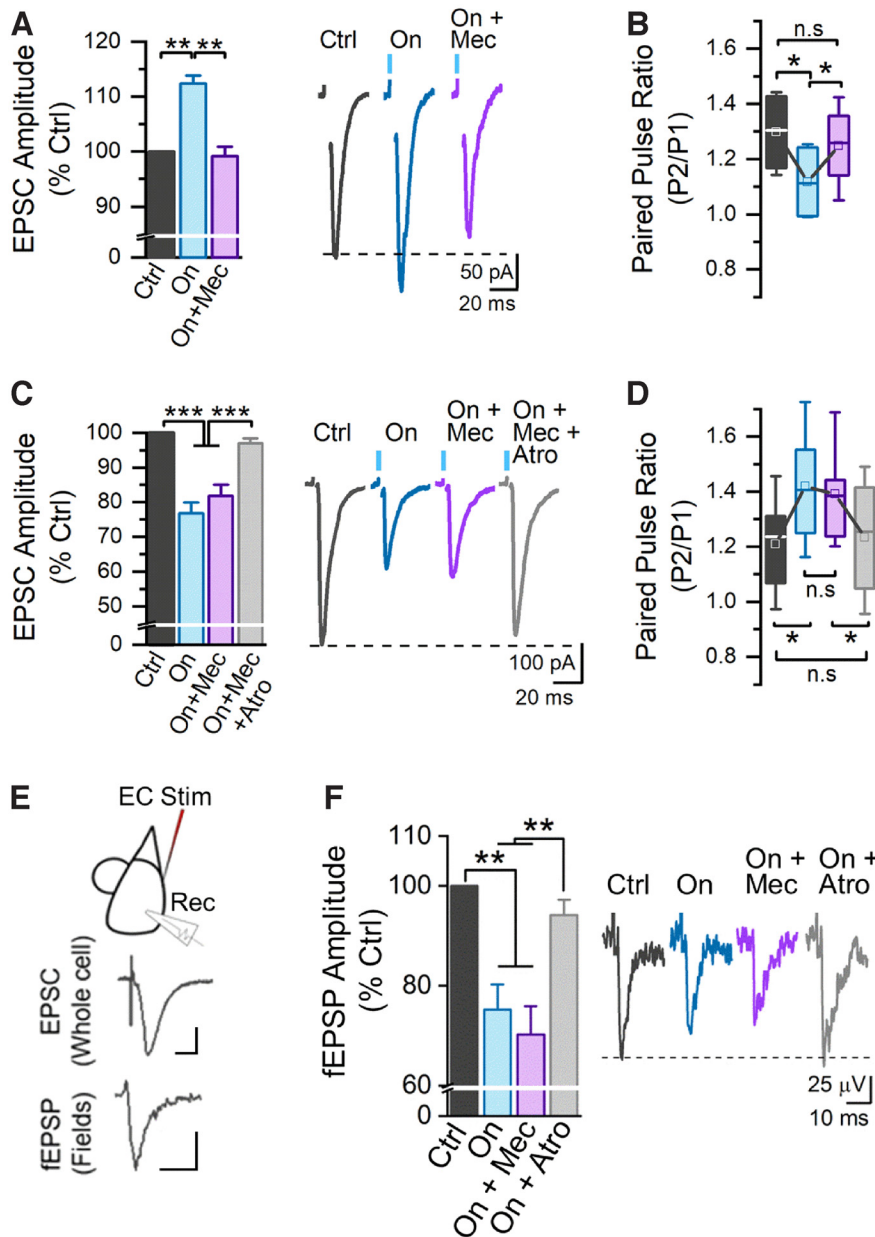


Figure 3. Released ACh regulates glutamatergic input to the BLA through presynaptic nicotinic and muscarinic receptors. **A**, Mecamylamine (Mec, $10 \mu\text{M}$) blocks facilitation of the EPSC at the early interval, indicating that this facilitation is nAChR-mediated ($n = 12$; $N = 8$; one-way repeated-measures ANOVA, $F_{(1,283,14,115)} = 13.81$; $p = 0.0013$). **B**, At the early interval, ACh-induced reduction of the paired pulse ratio is reversed by Mec ($n = 5$; $N = 5$; one-way repeated-measures ANOVA, $F_{(2,6)} = 5.68$; $p = 0.0413$). **C**, Cholinergic inhibition of the EPSC at the late interval is blocked by atropine (Atro; $5 \mu\text{M}$), but not Mec ($n = 11$; $N = 10$; one-way repeated-measures ANOVA, $F_{(3,30)} = 43.75$; $p = 4.510 \times 10^{-11}$). **D**, At the late interval, the ACh-evoked increase in the paired pulse ratio is reversed by atropine ($n = 5$; $N = 5$; one-way repeated-measures ANOVA, $F_{(3,12)} = 7.51$; $p = 0.0043$). **E**, Top, Schematic illustrating placement of the stimulating electrode in EC and recording electrode in BLA. EC stimulation evoked an EPSC when recording from a BLA pyramidal neuron (middle) or a fEPSP (bottom) when recording from an extracellular field electrode. Calibration: 75 pA , $75 \mu\text{V}$, 10 ms . **F**, Optogenetic activation of cholinergic terminals produced an atropine-sensitive inhibition of the fEPSP evoked by EC stimulation 250 ms later ($n = 7$; $N = 7$; one-way repeated-measures ANOVA, $F_{(3,18)} = 16.58$; $p = 2.025 \times 10^{-3}$). $*p < 0.05$. $**p < 0.01$. $***p < 0.001$.

fEPSP (Fig. 4B). This inhibition was blocked by atropine ($5 \mu\text{M}$), indicating that it was mediated by muscarinic receptors. Subsequent application of mecamylamine ($10 \mu\text{M}$) had no additional effect, suggesting that nicotinic receptors were not involved. In contrast, at the same recording site, elevation of ACh with physostigmine had no significant effect on baseline responses to MTN pathway stimulation. However, application of atropine significantly increased the MTN fEPSP,

and this increase was blocked by mecamylamine. These findings suggest that, at baseline, elevated ACh engaged both muscarinic and nicotinic receptors at MTN inputs to produce opposing and offsetting effects on the fEPSP. Application of atropine blocked the muscarinic inhibition, revealing the unopposed nicotinic facilitation which was subsequently blocked by mecamylamine. These differences in response to physostigmine in the two pathways could be caused, in part, by differences in the electrical versus optical method of stimulation. To evaluate this possibility, we examined the effect of physostigmine on fEPSPs evoked by optogenetic stimulation of PL inputs to BLA. These experiments were conducted in a separate group of mice that had been injected in PL cortex 4 weeks earlier with an rAAV containing ChR2-EYFP under the control of the CaMKII promoter. Results from these optogenetic experiments (Fig. 4B, right) were similar to results obtained using electrical stimulation of cortical input, indicating that differences in the effect of physostigmine in the two pathways is not caused by differences in the stimulation method. Overall, these findings reveal distinct effects of muscarinic and nicotinic receptors in cortical and MTN pathways. During sustained elevation of ACh, cortical input was strongly inhibited by muscarinic receptors, but little affected by nicotinic receptors. In contrast, thalamic input was more strongly facilitated by nicotinic receptors with markedly less muscarinic inhibition than at cortical inputs.

Differential regulation of cortical and thalamic input to the BLA by muscarinic receptors

To better examine pathway-specific differences in the effect of ACh, we injected an rAAV containing ChR2-EYFP under the control of the CaMKII promoter into either the PL or the MTN of mice. After 3–4 weeks, brain slices were prepared and the effect of muscarine, a selective mAChR agonist, on fEPSPs evoked by a single blue light pulse to either PL or MTN terminals in the BLA was examined. Muscarine ($10 \mu\text{M}$) inhibited fEPSPs in both the PL and MTN pathways with no sex-dependent difference at either input (% Control; PL males $18.2 \pm 2.2\%$ ($n = 26$, $N = 26$); female $20.8 \pm 4.2\%$ ($n = 6$, $N = 6$), $p = 0.6$, Student's t test; MTN males $51.8 \pm 6.4\%$ ($n = 14$, $N = 14$), female $39.2 \pm 4.5\%$ ($n = 13$, $N = 13$), $p = 0.13$, Student's t test) so data were collapsed across males and females for all experiments. Increasing concentrations of muscarine (0.03 – $30 \mu\text{M}$) produced a monotonic decrease in the amplitude of the fEPSP at both inputs (Fig. 5A). The effect of muscarine on PL-evoked fEPSPs could be fit to a standard logistic equation yielding an IC_{50} of $0.56 \mu\text{M}$ (95% CI

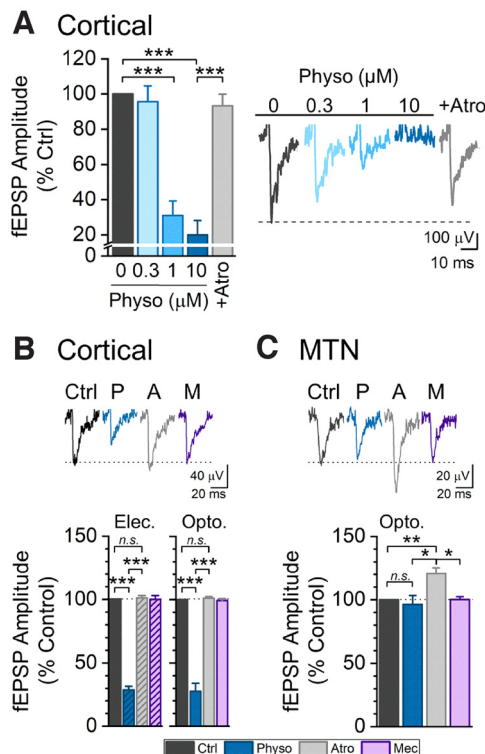


Figure 4. Pathway-specific regulation of afferent input to BLA by sustained ACh. **A**, Physostigmine (Physo) inhibits the EC-evoked fEPSP in a concentration-dependent manner. This inhibition is reversed by atropine (0.3 μM Physo: $n = 7$, $N = 7$, 1 μM Physo: $n = 5$, $N = 5$; 10 μM Physo: $n = 5$, $N = 5$; 5 μM atropine: $n = 4$, $N = 4$; one-way ANOVA, $F_{(4,23)} = 28.73$; $p = 1.1988 \times 10^{-8}$). **B**, Physo (10 μM) similarly inhibits the cortical fEPSP evoked by electrical EC stimulation (left, hatched) or optogenetic stimulation of PL inputs (right). This inhibition is blocked by Atr (5 μM), but unaffected by Mec (10 μM), indicating a role for mAChRs, but not nAChRs (electrical stimulation [left, hatched]: one-way repeated-measures ANOVA, $F_{(3,9)} = 176.25$; $p = 2.607 \times 10^{-8}$; optogenetic stimulation [right]: one-way repeated-measures ANOVA, $F_{(3,12)} = 123.24$; $p = 2.79 \times 10^{-9}$). **C**, In the same brain slices as the electrical EC stim in **B**, Physo had little effect on the fEPSP evoked by optogenetic stimulation of MTN input. In contrast, Atr blocked mAChRs, revealing an underlying potentiation that was subsequently inhibited by Mec (one-way ANOVA, $F_{(3,22)} = 5.934$; $p = 0.0039$). These results suggest that, at MTN synapses, the elevation of ACh produced by Physo engaged both nAChRs and mAChRs to produce opposing and offsetting effects. During sustained elevation of ACh, mAChR inhibition is stronger at cortical input, whereas nAChR-mediated facilitation is stronger at MTN input. * $p < 0.05$. ** $p < 0.01$. *** $p < 0.001$.

0.38–0.80 μM) and Hill coefficient of 0.58 (95% CI 0.48–0.68; $n = 5$ –35 slices). Similar analysis of the MTN-evoked fEPSP indicated that the effect of muscarine in this pathway was shifted ~10 fold to the right ($IC_{50} = 6.04$ (95% CI 3.66–9.23 μM), Hill coefficient = 0.56 (95% CI 0.40–0.79; $n = 4$ –27). The CIs of the IC_{50} concentrations at these two inputs did not overlap indicating that PL input was significantly more sensitive to inhibition by muscarine than was MTN input.

Input to BLA from ventral subiculum (vSub) also plays an important role in regulating amygdalar responses to emotionally arousing stimuli. Given the differing effects of muscarine at PL and MTN inputs, we also assessed muscarine inhibition of input from vSub. fEPSPs were evoked by optogenetic stimulation of vSub terminals in BLA 4 weeks after injection into vSub of AAV containing Chr2-EYFP. Muscarine (10 μM) strongly inhibited these fEPSPs, similar to its effect on PL-evoked fEPSPs, but significantly greater than its inhibition of MTN inputs (Fig. 5B). As observed following EC stimulation (Fig. 3D), the effect of muscarine on both PL and MTN inputs was presynaptic, since muscarine significantly enhanced the paired pulse ratio in both

pathways (Fig. 5C,D). Together, these results indicate the presynaptic nature of muscarinic inhibition and that PL and vSub input to BLA are significantly more sensitive to this inhibition than MTN input.

ACh acts via M3 and M4 receptors to suppress transmission

To identify the mAChR subtype(s) involved in the muscarine-mediated inhibition of the PL- and MTN-evoked fEPSP, we used a protocol in which 10 min of baseline recording was followed by perfusion with muscarine (10 μM) to inhibit the fEPSP before addition of selective muscarinic receptor antagonists. Each drug was perfused until a steady-state effect was observed before moving to the next drug. PL or MTN inputs were optogenetically stimulated, and AMPAR fEPSPs were isolated using 10 μM picrotoxin, 2 μM CGP55845, and 50 μM APV or 10 μM MK-801 to block GABA and NMDA receptors. M1 receptors are the most abundant mAChR in the BLA and have been reported to be present at presynaptic glutamatergic terminals (Muller et al., 2013). However, at both the PL and MTN inputs, the selective M1 receptor antagonist, telenzepine (100 nM; $pK_i = 8.46$), at a concentration shown to inhibit the effects of muscarine (10 μM) in other systems (Christofi et al., 1991; Liu et al., 1998), had no significant effect on the fEPSP in the presence of muscarine. To further rule out a role for M1 receptors, we tested the effect of VU0255035 (5 μM; $pK_i = 7.8$), a selective M1 receptor antagonist with >75-fold selectivity over M2–M5 receptors (Sheffler et al., 2009). VU0255035 ($IC_{50} = 132.6 \pm 28.5$ nM) was used at a concentration has been reported to block carbachol (CCh, 10 μM)-induced potentiation of NMDA currents (Sheffler et al., 2009) and CCh-induced neuronal depolarization (Xiang et al., 2012; Kurowski et al., 2015), demonstrating its effectiveness. Nevertheless, like telenzepine, VU0255035 also did not produce significant reversal of muscarinic inhibition in either pathway. Consequently, the effect of these two antagonists was combined (Fig. 6A,B) and indicated little functional involvement of M1 receptors in the muscarinic inhibition. The involvement of M2 receptors was tested using the highly selective M2 receptor antagonist AF-DX 116 ($pK_i = 6.7$). AF-DX 116 (0.1–1 μM) blocks ACh (10 μM)-induced inhibition of transmitter release in hippocampus (Raiteri et al., 1990; Goswamee and McQuiston, 2019) and CCh induced suppression of EPSPs in cortex (Gigout et al., 2012). However, in BLA, AF-DX 116 (1 μM) had no effect on muscarinic inhibition of fEPSPs in either pathway (Fig. 6A,B), indicating that M2 receptors were not involved.

In contrast, the M3 antagonist 4-DAMP (1 μM, $pK_i = 9.3$) completely reversed muscarinic inhibition at both pathways to the BLA (Fig. 6A,B). While 4-DAMP is considered an M3 antagonist, it shows limited selectivity over M1, M4, and M5 receptors (Dorje et al., 1991; Moriya et al., 1999; Watson et al., 1999). However, the inability of selective M1 or M2 receptor antagonists to block muscarinic inhibition and the lack of evidence supporting M5 receptors in the BLA (Lebois et al., 2018) suggest that 4-DAMP must block muscarinic inhibition by acting on either M3 or M4 receptors.

To investigate any contribution of M4 receptors to inhibition at PL and/or MTN input, we used the highly selective M4-positive allosteric modulator (M4 PAM) VU0467154 (VU154). In these experiments, a low dose of muscarine (0.3 μM) was initially applied followed by VU154 (3 μM). At the PL pathway, inhibition by this low dose of muscarine was significantly enhanced after application of the M4 PAM (Fig. 6C), indicating that presynaptic M4 receptors are present on PL terminals and inhibit glutamatergic transmission in this pathway. VU0154 (3 μM) also facilitated inhibition produced

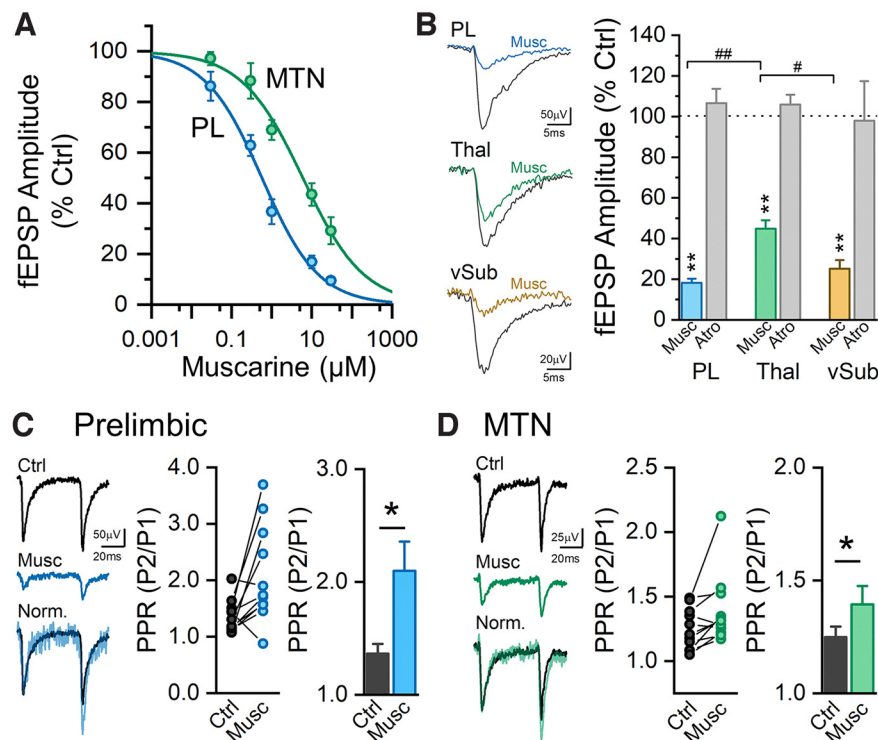


Figure 5. Stimulation of presynaptic muscarinic receptors more strongly inhibits cortical and subicular projections, than MTN projections to the BLA. **A**, Effect of muscarine (0.3–10 μM) on the fEPSP evoked by optogenetic stimulation of either pre-limbic or MTN input to BLA. Muscarine produced a concentration-dependent inhibition of the fEPSP in both pathways. The inhibitory effect of muscarine in the MTN pathway was shifted significantly to the right (PL Input, $n = 5$ –35; MTN input, $n = 4$ –27). **B**, Selective optogenetic stimulation of PL, MTN, or vSub input to the BLA evoked a fEPSP which was inhibited by muscarine (10 μM). Muscarine produced significantly greater inhibition of PL and vSub, than MTN input (PL, $n = 32$, $N = 27$; MTN, $n = 26$, $N = 22$; vSub, $n = 5$, $N = 5$; one-way ANOVA, $F_{(2,60)} = 20.10$; $p = 2.086 \times 10^{-7}$). **C**, **D**, Muscarine inhibited the first fEPSP but significantly enhanced paired pulse facilitation (50 ms interstimulus interval) at both the PL ($n = 11$; $N = 11$; Student's t test, $p = 0.016$) and MTN inputs ($n = 11$; $N = 11$; Student's t test, $p = 0.031$), indicating a presynaptic site of action in each pathway. * $p < 0.05$. ** $p < 0.01$. # $p < 0.05$. ## $p < 0.01$.

by another muscarinic agonist, oxotremorine. The M4 PAM increased oxotremorine (0.3 μM)-induced inhibition from $18.7 \pm 2.8\%$ in baseline to $60.4 \pm 8.6\%$ in the presence of the M4 PAM ($n = 5$; $N = 5$; $p = 0.013$, paired t test). In contrast, the M4 PAM had no effect on either muscarine-induced (Fig. 6D) or oxotremorine (5 μM)-induced inhibition ($18.9 \pm 2.5\%$ inhibition in oxotremorine, $18.2 \pm 1.1\%$ inhibition in oxotremorine + VU154; $n = 3$; $N = 3$; $p = 0.76$, paired t test) at the MTN input. Together, these experiments suggest that M4 receptors contribute to muscarinic inhibition at PL input to BLA, while inhibition at MTN inputs is exclusively mediated by M3 receptors.

Muscarine inhibits synaptic transmission in the PL pathway through Gi/o protein-coupled M4 mAChRs

Because M3 receptors couple to Gq proteins and M4 receptors to Gi/o proteins, treating slices with an agent that inhibits Gi/o proteins should distinguish between inhibitory effects mediated by M3 and M4 receptors. Therefore, to further confirm a role for M4 receptors in producing inhibition in the PL pathway, we assessed the effect of Gi/o protein inactivation by bath application of the sulfhydryl alkylating agent *n*-ethylmaleimide (NEM) on the effects of muscarine (Shapiro et al., 1994; Morishita et al., 1997). Baclofen, a GABA_B receptor agonist that inhibits glutamate release through a Gi/o-coupled mechanism in the BLA (Yamada et al., 1999), served as a positive control. As expected,

baclofen (10 μM) significantly inhibited the fEPSP evoked by optogenetic stimulation of the PL input, and this inhibition was reversed by the selective GABA_B antagonist, CGP55845 (2 μM , Fig. 7A). In separate experiments, we then used a protocol in which 10 min of baseline recording was followed by perfusion with muscarine (10 μM) to inhibit the PL-evoked fEPSP and establish the baseline level of muscarinic inhibition. Muscarine was then washed out and NEM (50 μM) (Shapiro et al., 1994) was bath-applied to slices for a minimum of 15 min. Muscarine (10 μM) was again applied, and the amplitude of the fEPSP after NEM treatment was compared with the fEPSP amplitude before NEM treatment. Baclofen (10 μM) was also applied following NEM treatment as a positive control and the extent of inhibition compared with that produced by baclofen in the absence of NEM in additional brain slices from the same animals. Incubation of slices with NEM was sufficient to inactivate Gi/o proteins, as effects of baclofen were significantly inhibited (Fig. 7B). Similar to its effects on baclofen inhibition, NEM also blocked muscarine inhibition (Fig. 7B). The similarity in the effect of NEM on baclofen and muscarine inhibition suggests that both agents act at PL input through Gi/o protein-dependent mechanisms and supports the conclusion that muscarine inhibits glutamate release at PL input through Gi/o-coupled presynaptic M4 receptors.

Muscarinic inhibition in the PL and MTN pathways occurs through mechanisms independent of GABA_B receptors

An alternative explanation for the above findings is that muscarine acts on M3 receptors on GABAergic interneurons to increase interneuron excitability, releasing GABA, which acts on GABA_B receptors to suppress synaptic transmission. This mechanism has recently been reported in hippocampal area CA1 (Goswamee and McQuiston, 2019). NEM would suppress this effect by blocking the action of Gi/o protein-coupled GABA_B receptors. However, as our experiments are performed in the presence of picrotoxin and CGP55845, GABA_A and GABA_B receptors were not required for muscarinic inhibition at PL or MTN inputs to BLA. To determine whether muscarinic inhibition was greater when GABA_B receptors were available, we compared the extent of inhibition by muscarine in the absence and presence of CGP55845. Bath application of CGP55845 (2 μM) had no effect on muscarine inhibition in either pathway, indicating that, although presynaptic GABA_B receptors are present, muscarine suppression of glutamatergic fEPSPs at PL and MTN inputs is independent of GABA_B receptors (Fig. 7C,D). Similarly, in whole-cell experiments, blockade of GABAergic inhibition by addition of picrotoxin (50 μM) and CGP55845 (5 μM) did not alter either the early facilitation (ACSF, $111.3 \pm 2.8\%$ vs GABA blockers, $110.7 \pm 2.0\%$, $n = 3$, $p = 0.87$, paired t test) or late

inhibition (ACSF, $84.5 \pm 3.3\%$ vs GABA blockers, $82.2 \pm 3.7\%$, $n = 5$, $p = 0.2$, paired t test) produced by stimulation of cholinergic terminals, indicating that ACh did not act through GABAergic mechanisms to produce its effects.

Muscarine inhibits MTN inputs through an M3 receptor-dependent facilitation of retrograde endocannabinoid (eCB) signaling

eCBs serve a retrograde inhibitory role in many brain regions (Ohno-Shosaku and Kano, 2014), allowing neurons to regulate their upstream neuronal inputs. Postsynaptic Gq-coupled muscarinic (M1/M3) receptors can facilitate retrograde eCB release, suppressing GABA (Kim et al., 2002; Ohno-Shosaku et al., 2003) or glutamate transmission (Chiu and Castillo, 2008; Kodirov et al., 2009). While this mechanism has not previously been reported at excitatory terminals in the BLA, it is possible that postsynaptic M3 receptors on BLA pyramidal cells could act through retrograde eCB release to inhibit glutamatergic transmission in the MTN or PL pathway. To examine this possibility, the selective CB1 antagonist, AM251 ($1 \mu\text{M}$), was applied in the presence of muscarine. At PL input, antagonism of CB1 receptors had no effect on muscarine inhibition (Fig. 8A). This lack of effect was somewhat surprising given the presence of CB1 receptors at these inputs, as application of CB1 receptor agonist WIN55212 ($5 \mu\text{M}$) suppressed PL-evoked fEPSPs in a manner reversible by AM251 (Fig. 8B). These data suggest that, although CB1 receptors can inhibit PL evoked fEPSPs in the BLA, muscarinic suppression of PL input is not CB1 receptor-dependent. Given the presence of CB2 receptors in the brain (Onaivi et al., 2008) and the ability of CB2 receptors to suppress transmitter release in some brain regions (Foster et al., 2016), in separate experiments, we also tested the effect of the CB2 antagonist, AM630. However, as with CB1 antagonists, AM630 ($2 \mu\text{M}$) had no effect on muscarine inhibition (Musc: $30.1 \pm 5.2\%$; Musc + AM630: $27.7 \pm 2.0\%$; $n = 3$; $N = 3$; $p = 0.75$, paired t test). In contrast, at MTN inputs blockade of CB1 receptors with AM251 completely reversed muscarinic inhibition of fEPSPs (Fig. 8C), while having no effect on baseline fEPSPs in the absence of muscarine (Fig. 8D). Muscarine inhibition at MTN input is dependent on M3 receptors (Fig. 6). These findings suggest that at MTN inputs, muscarine inhibition is mediated by a postsynaptic M3 receptor-mediated release of eCBs, which retrogradely acts on CB1 receptors on MTN terminals to inhibit glutamatergic transmission (Fig. 8E).

Frequency-dependent inhibition of glutamatergic input by mAChRs

PL and MTN inputs are differentially modulated by mAChRs in response to single pulse stimulation. However, theta (4–12 Hz) and γ (30–80 Hz) frequency activity occurs in the BLA during emotional behavior and associative learning (Stujenski et al., 2014; Bocchio et al., 2017), making it of considerable interest to understand how ACh regulates afferent synaptic transmission at different frequencies in each pathway. Therefore, we investigated the effect of muscarine on responses in PL and MTN pathways to short stimulus trains at frequencies within a behaviorally relevant range *in vivo*. Stimulus trains consisting of 10 light pulses were delivered to either input at frequencies ranging from 1 to 40 Hz in the absence or presence of muscarine ($10 \mu\text{M}$). At PL synapses, stimulation at 1 Hz evoked responses of similar amplitude throughout the train. Muscarine ($10 \mu\text{M}$) strongly and similarly suppressed each response of the train (Fig. 9A,B). Alternately, stimulation at 40 Hz evoked a

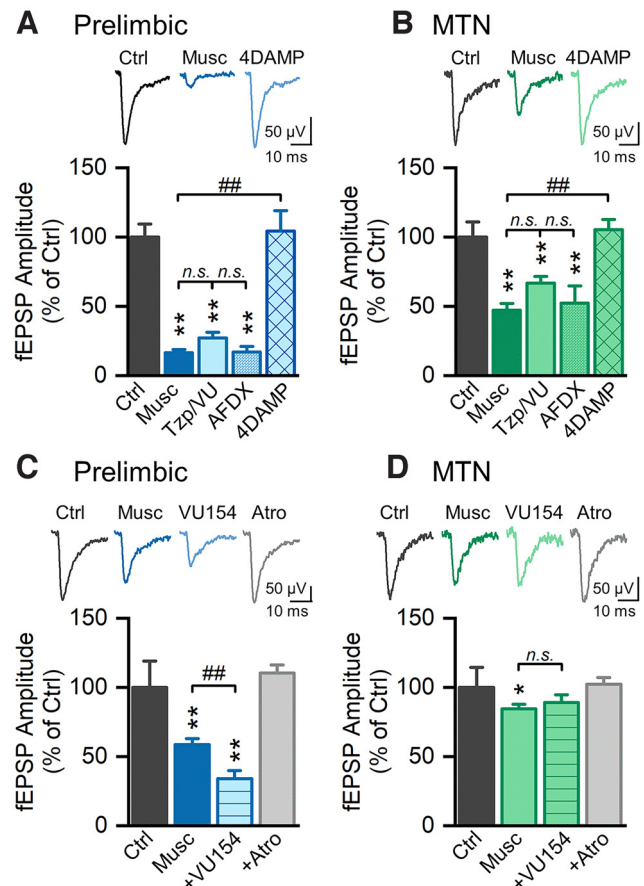


Figure 6. M3 and M4 mAChRs differentially regulate glutamatergic synaptic transmission from PL and MTN to the BLA. **A**, Antagonism of M1 receptors with telenzepine (Tzp, 100 nM , $27.8 \pm 6.5\%$, $n = 6$, $N = 6$) or VU0255035 (VU035, $5 \mu\text{M}$, $25.8 \pm 1.4\%$, $n = 3$, $N = 3$) failed to reduce muscarine ($10 \mu\text{M}$) inhibition of PL input. Given the similarity in the lack of effect of these antagonists (Tzp $27.8 \pm 6.5\%$ of baseline; VU035 $25.8 \pm 1.4\%$ of baseline), the results were combined. Antagonism of M2 receptors with AF-DX 116 ($1 \mu\text{M}$) also failed to reverse muscarinic inhibition of the fEPSP ($n = 6$; $N = 6$). In contrast, the M3/M4 antagonist 4DAMP ($1 \mu\text{M}$) blocked muscarinic inhibition ($n = 10$; $N = 10$; one-way ANOVA, $F_{(5,94)} = 45.90$; $p = 0.0000$), indicating that M3 or M4 receptors were responsible for inhibition in the PL pathway. **B**, At MTN input, muscarine ($10 \mu\text{M}$) produced less inhibition than at PL input. However, as at PL input, this inhibition was not reduced by M1 antagonists (Tzp or VU035, $n = 6$, $N = 6$) or the M2 antagonist AF-DX 116 ($n = 5$, $N = 5$), but was reversed by 4-DAMP ($n = 9$, $N = 9$; one-way ANOVA, $F_{(5,74)} = 31.48$; $p = 0.0000$), indicating that M3 or M4 receptors were responsible. **C**, The M4 PAM, VU0467154, significantly potentiated inhibition produced by $0.3 \mu\text{M}$ muscarine in the PL pathway ($n = 8$, $N = 8$; one-way repeated-measures ANOVA, $F_{(3,21)} = 57.69$; $p = 2.5996 \times 10^{-10}$), indicating a role for presynaptic M4 receptors. **D**, In contrast, at MTN input, muscarine ($0.3 \mu\text{M}$) produced a small but significant inhibition ($n = 4$, $N = 4$; one-way repeated-measures ANOVA, $F_{(3,9)} = 8.95$; $p = 0.0046$), and the M4 PAM did not potentiate this inhibition ($p = 0.69$, *post hoc* Tukey test), indicating that muscarine produced inhibition in this pathway by acting on M3 receptors. * $p < 0.05$. ** $p < 0.01$. ## $p < 0.01$.

facilitation on the second response of the train (Fig. 9A,B) in line with earlier results showing paired pulse facilitation in this pathway (Figs. 3 and 5). Subsequent pulses in the train evoked progressively smaller fEPSPs such that the last fEPSP was $35.5 \pm 2.8\%$ of the amplitude of the first fEPSP. Following addition of muscarine, the first response of the train was strongly inhibited, as seen with single pulses, but subsequent responses were facilitated relative to the first fEPSP. This facilitation was maintained throughout the remainder of the train, such that the fEPSP amplitude in response to the last pulse of the train in muscarine was similar to the fEPSP amplitude to the last pulse in control (Fig. 9A,B), reflecting a complete loss

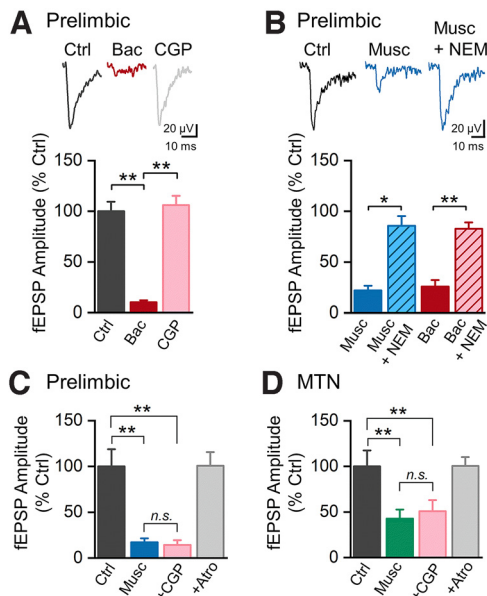


Figure 7. Mechanisms of muscarinic inhibition. **A, B**, Muscarine inhibition of PL input is dependent on Gi/o protein-dependent signaling. **A**, Baclofen (10 μ M), which acts via GABA_B receptors coupled to Gi/o proteins, inhibits fEPSPs evoked by optogenetic stimulation of the PL pathway. This inhibition is reversed by the GABA_B receptor antagonist, CGP55845 (CGP, 2 μ M, $n = 7$, $N = 7$; one-way repeated-measures ANOVA, $F_{(1,029,6,172)} = 92.12$; $p = 5.93 \times 10^{-5}$). **B**, Treatment of brain slices with NEM (50 μ M) for 15 min inactivated Gi/o proteins and blocked muscarine (10 μ M) inhibition in the PL pathway ($n = 4$, $N = 4$). In the same slices, NEM also blocked the inhibitory effect of baclofen (10 μ M) in this pathway, demonstrating that Gi/o proteins were inactive ($n = 4$, $N = 4$; one-way ANOVA, $F_{(4,15)} = 37.64$; $p = 1.18 \times 10^{-7}$). These findings suggest that muscarine inhibition in the PL pathway is dependent on Gi/o protein-coupled M4 receptors, rather than Gq protein-coupled M3 receptors. **C, D**, An alternative interpretation of these data is that muscarine produces inhibition indirectly through an M3 muscarinic receptor-mediated increase in inhibitory interneuron excitability, which activates GABA_B receptors to suppress synaptic transmission. NEM would then block muscarine inhibition by blocking GABA_B receptor signaling. However, application of CGP55845 (2 μ M) did not block muscarine inhibition in either the PL (2 μ M, $n = 6$, $N = 6$; one-way repeated-measures ANOVA, $F_{(1,077,5,385)} = 30.81$; $p = 0.0019$) or MTN pathway (2 μ M, $n = 5$, $N = 5$; one-way repeated-measures ANOVA, $F_{(3,12)} = 28.36$; $p = 9.89 \times 10^{-6}$). These findings indicate that muscarinic inhibition of PL and MTN inputs to BLA is not dependent on GABA_B receptors. * $p < 0.05$. ** $p < 0.01$.

of muscarine inhibition during the train. When comparing the extent of muscarine inhibition on the last pulse of different frequency trains, it could be seen that muscarine inhibition during the train was frequency-dependent (Fig. 9C). Inhibition was preserved during low-frequency 1 Hz stimulation, but increasingly attenuated as the frequency of the train increased. At 40 Hz, a frequency in the γ range, inhibition was completely lost during the train. A similar result was also found at MTN input. As seen with single pulses, muscarine inhibition was significantly less in this pathway compared with PL input. However, as in the PL pathway, this muscarine inhibition was preserved during low-frequency (1–5 Hz) trains, but attenuated during trains with frequencies > 5 Hz, reaching a complete loss of inhibition at 40 Hz. Thus, at both PL and MTN inputs, muscarinic receptors act as a high pass filter, blocking low-frequency signals, while allowing higher-frequency signals to reach the BLA.

Discussion

Our results show robust ACh regulation of afferent input to BLA that is pathway-specific and frequency-dependent. ACh released by single pulse stimulation of cholinergic terminals engaged both nAChRs and mAChRs, producing a biphasic

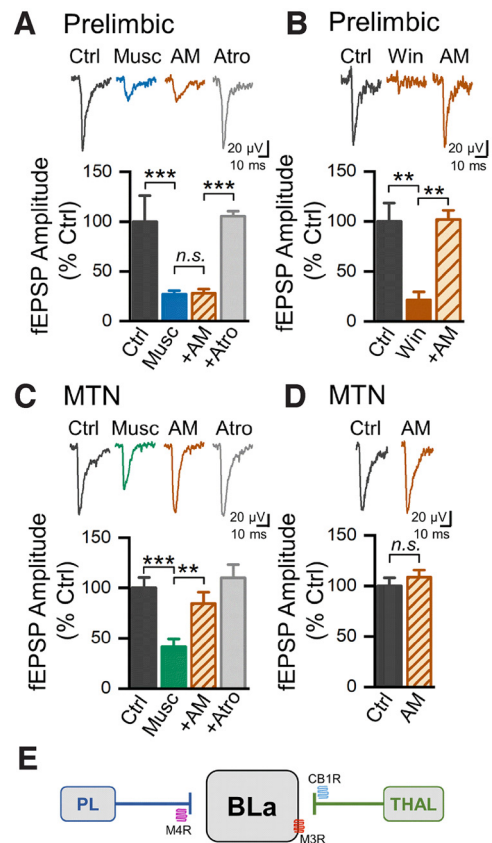


Figure 8. Muscarinic inhibition of MTN, but not PL input, is mediated by an M3 receptor-dependent facilitation of retrograde eCB signaling. **A**, The CB1 receptor antagonist, AM251 (AM, 1 μ M), had no significant effect on muscarine (10 μ M) inhibition in the PL pathway. Muscarine inhibition was completely reversed by atropine (5 μ M, $n = 6$, $N = 6$; one-way repeated-measures ANOVA, $F_{(3,15)} = 209.96$; $p = 1.803 \times 10^{-12}$). **B**, The CB1 agonist, Win 55212-2 (5 μ M) strongly suppressed fEPSPs at PL inputs. This suppression was reversed by AM251, indicating that it was dependent on CB1 receptors ($n = 6$, $N = 6$; one-way repeated-measures ANOVA, $F_{(2,6)} = 20.31$; $p = 0.0021$). These findings suggest that CB1 receptors are present at PL terminals but are not engaged during muscarinic inhibition. **C**, In contrast, at MTN input, AM251 (1 μ M) reversed muscarine inhibition ($n = 7$, $N = 7$; one-way repeated-measures ANOVA, $F_{(3,18)} = 16.46$; $p = 2.12 \times 10^{-5}$). Subsequent addition of atropine had no additional significant effect (Tukey *post hoc* test, $p = 0.26$). **D**, AM251 by itself had no significant effect on the optogenetically evoked fEPSP at the MTN input ($n = 3$, $N = 3$, $p = 0.34$, paired *t* test), indicating that AM251 did not directly facilitate synaptic transmission in this pathway. Together, these results suggest that muscarine inhibits responses in the MTN pathway by acting on postsynaptic M3 receptors to facilitate retrograde eCB release which acts on presynaptic CB1 receptors on MTN terminals. ** $p < 0.01$. **E**, Summary of the differing sites of action of M3 and M4 muscarinic receptors at PL and MTN inputs to BLA.

excitatory-inhibitory modulation of cortical input in the BLA. By contrast, elevation of extracellular ACh by blockade of acetylcholinesterase produced solely monophasic muscarinic inhibition of cortical input. At thalamic input in the same brain slices, this increase in extracellular ACh had no net effect on synaptic transmission. The differences in sensitivity of cortical and thalamic inputs to muscarinic inhibition were attributed to distinct mechanisms of mAChR action at each site. Muscarine inhibition at both inputs disappeared at higher frequencies of stimulation, consistent with its action as a high pass filter for afferent BLA signals.

Pharmacological studies with persistent agonist application have demonstrated nicotinic and muscarinic receptor regulation of transmitter release in the BLA (Sugita et al., 1991; Yajeya et al., 2000; Jiang and Role, 2008). The present study extends those findings by showing rapid regulation of

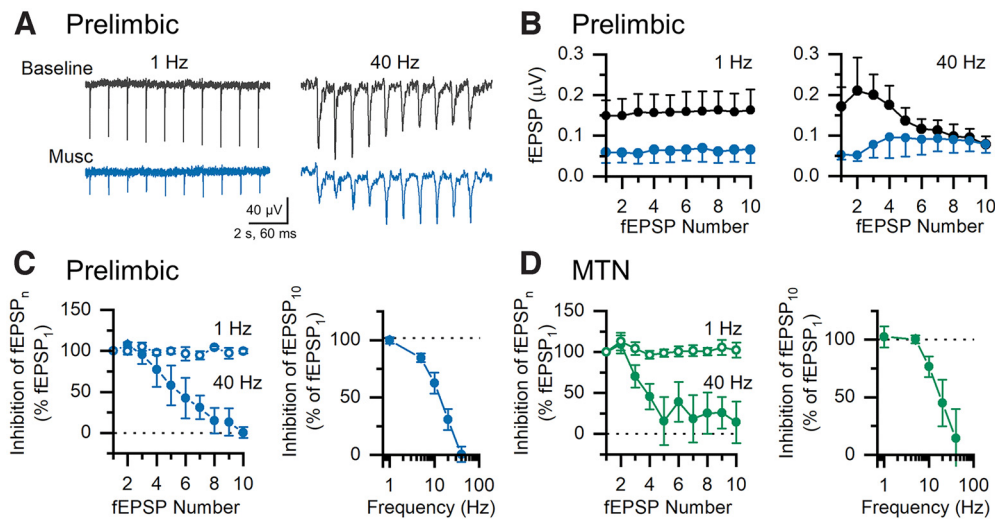


Figure 9. Muscarine inhibition at PL and MTN inputs is frequency-dependent. **A, B**, Optogenetic stimulation of PL input at 1 Hz evoked fEPSPs that were consistently inhibited by muscarine (10 μ M) during the stimulus train. During 40 Hz stimulation, fEPSPs in baseline initially facilitated, then became progressively smaller. In muscarine, fEPSPs were initially strongly inhibited. They then facilitated for the remainder of the train such that, by the end of the train, the fEPSP in muscarine was the same amplitude as in control, reflecting a loss of muscarine inhibition ($n = 4$, $N = 4$). **C**, At low frequency (1 Hz), muscarine inhibition was stable during the train. At high frequency (40 Hz), muscarine inhibition progressively declined with subsequent pulses until it was completely absent by the end of the train. Muscarine inhibition at the end of the 10 pulse stimulus train progressively declined at higher stimulus frequencies. **D**, A similar frequency dependence of muscarine inhibition was also observed at MTN input ($n = 6$, $N = 6$).

glutamatergic transmission by endogenously released ACh. These findings are consistent with anatomic studies showing cholinergic terminals converging on glutamatergic synapses in BLA (Li et al., 2001; Muller et al., 2011). Single pulse stimulation of cholinergic terminals produced an immediate (<20 ms) and short-lived nAChR-mediated facilitation of cortical input to BLA, followed by a slower mAChR-mediated inhibition, lasting for up to 1 s. Both facilitation and inhibition of afferent input were evoked by the same single cholinergic stimulus. Prior studies have reported postsynaptic responses to individual cholinergic stimuli in inhibitory neurons in thalamus and cortex (Sun et al., 2013; Urban-Ciecko et al., 2018). However, to our knowledge, this is the first study that demonstrates that ACh release can potentiate glutamate release on the timescale of an individual synaptic event. This is also the first demonstration of this form of excitatory-inhibitory neuromodulation by ACh in the amygdala and suggests that cholinergic neuromodulation can serve precise, computational roles in the BLA network. The presence of these forms of cholinergic modulation in BLA is consistent with the robust cholinergic innervation of this region and further supports the vital role of ACh in information processing in this region.

Cholinergic neurons in BF exhibit fast and precise responses to both appetitive and aversive behavioral cues (Hangya et al., 2015). Studies using fluorescent ACh sensors have found that, during emotionally salient stimuli, phasic release of ACh into the BLA (Crouse et al., 2020) mediates associative learning (Jiang et al., 2016). In addition, phasic BF cholinergic stimulation can induce acute appetitive behaviors (Aitta-aho et al., 2018). It is tempting to speculate that the excitatory-inhibitory modulation of glutamatergic transmission by endogenously released ACh observed here underlies the action of phasically released ACh in the BLA during these behaviors. Phasic ACh rapidly engaged nAChRs on cortical terminals in BLA to facilitate glutamate release for up to 20 ms following cholinergic terminal activation. In contrast, glutamate release 50–1000 ms after stimulation of cholinergic inputs was suppressed by robust mAChR-mediated inhibition. Together, the biphasic

action of endogenously released ACh on presynaptic nicotinic and muscarinic receptors suggests that it would entrain glutamatergic input in a tight temporal window following cholinergic terminal activation and suppress poorly timed input that arrived outside of this window. This mechanism would enhance the signal-to-noise ratio for cortical input to BLA, thereby facilitating attention to salient signals (Bloem et al., 2014; Dannenberg et al., 2017) and may be important in forms of heterosynaptic plasticity in the BLA (Jiang et al., 2016).

ACh release from the BF occurs at multiple physiological timescales, ranging from milliseconds to hours (Disney and Higley, 2020; Sarter and Lustig, 2020). To better understand the consequences of sustained ACh elevation on glutamate transmission, we increased extracellular ACh by inhibiting acetylcholinesterase with physostigmine. In contrast to phasic ACh, sustained ACh elevation produced a steady state and reversible monophasic inhibition of cortical input. This inhibition was concentration-dependent, such that ACh elevation produced by even a low concentration of physostigmine inhibited cortical input. The inhibition was also mAChR-mediated as it was entirely reversed by atropine and unaffected by nAChR blockade. The lack of nAChR involvement is likely attributed to nAChR desensitization during sustained ACh, which has been well documented for these receptors (Quick and Lester, 2002; Giniatullin et al., 2005). In contrast to its effects at cortical inputs, under the same conditions and in the same brain slices, sustained ACh elevation produced little net effect at MTN input. The lack of effect was associated with both a larger persistent nicotinic facilitation and a smaller muscarinic inhibition that opposed and occluded each other. The persistence of nAChR-mediated facilitation at MTN input during elevated ACh may reflect distinct nAChR types at MTN compared with PL synapses (Quick and Lester, 2002; Venkatesan and Lambe, 2020) or differences in the anatomic arrangement of cholinergic release sites and thalamic terminals (Disney and Higley, 2020). This could result in lower concentrations of ACh at MTN synapses which would be less likely to desensitize nAChRs.

In addition to differences in nicotinic facilitation, MTN synapses were also subject to significantly less muscarinic inhibition than PL input. This disparity was caused by differential regulation of transmitter release by M4 and M3 receptors at the two inputs. These findings are consistent with growing evidence of highly specific localization of muscarinic receptor types to distinct neural pathways in the brain (Gil et al., 1997; Palacios-Filardo et al., 2021). The finding that M4 receptors regulate PL input is the first demonstration of presynaptic inhibition by M4 receptors in the BLA and builds on prior work showing presynaptic regulation by M4 receptors in other brain regions (Dasari and Gullledge, 2011; Pancani et al., 2014; Yang et al., 2020; Palacios-Filardo et al., 2021). Inhibition by M4 receptors was likely mediated by a suppression of presynaptic N- and P-type voltage-gated calcium channels through a Gi/o protein-dependent mechanism (Hille, 1994; Howe and Surmeier, 1995; Yan and Surmeier, 1996). Blockade of muscarinic inhibition by NEM in the present study supports this conclusion (see also Shapiro et al., 1994). Muscarinic modulation of these calcium channels is voltage-dependent and is attenuated by membrane depolarization (Yan and Surmeier, 1996). This voltage dependence could underlie the observed loss of muscarinic inhibition during high-frequency stimulation when the presynaptic membrane would be depolarized. This mechanism could explain why low-frequency transmission at cortical inputs would be suppressed by presynaptic mAChRs, but high-frequency or burst transmission would pass. Presynaptic mAChRs would thereby serve as a high pass filter for incoming salient information from cortex.

In contrast, at MTN inputs muscarinic inhibition is mediated by M3 receptors. The differences in muscarinic receptor type at PL and MTN inputs provide a mechanism for differential sensitivity to ACh in these two pathways and are consistent with the finding that muscarine was significantly less potent at MTN than PL input. Our data indicate that ACh suppressed glutamate release at MTN inputs by acting on postsynaptic M3 receptors to stimulate retrograde eCB release which subsequently engaged CB1 receptors on thalamic terminals. This conclusion is supported by the ability of an M3 receptor antagonist to block the inhibition and the inability of muscarine to produce inhibition in the presence of a CB1 receptor antagonist. Muscarinic receptor-induced suppression of excitation has been reported (Chiu and Castillo, 2008; Kodirov et al., 2009) but has not been demonstrated in BLA. However, its role in this region is consistent with both the high expression of CB1 receptors in the amygdala (Marsicano and Lutz, 1999) and the presence of these receptors in glutamatergic terminals in this area (Domenici et al., 2006; Fitzgerald et al., 2019). Our data show that a CB1 receptor agonist suppressed transmission at both PL and MTN inputs, indicating the presence of CB1 receptors at both glutamatergic synapses. The presence of muscarinic receptor-induced suppression of excitation only at MTN input thus reflects the localization of M3 receptors capable of stimulating eCB release. These findings highlight the pathway-specific control of glutamate release by distinct cholinergic receptors and provide targets to selectively modulate individual components of ACh's actions.

The marked difference in muscarinic inhibition at PL and MTN inputs suggests that during behavioral states associated with high cholinergic tone, thalamic input will more strongly influence BLA activity than will cortical input. These findings are consistent with prior work in cortex showing that ACh enhances the influence of thalamic sensory input on cortical activity through a nicotinic facilitation of glutamate release,

and reduces internal corticocortical connections by presynaptic muscarinic inhibition (Hasselmo, 2006; Hasselmo and Sarter, 2011). The resulting reduction in cortical feedback excitation is postulated to reduce interference from previous retrieval and thereby enhance memory encoding and attention to novel sensory input. The differential cholinergic modulation of PL and MTN inputs seen in the present study may similarly favor thalamic sensory input and reduce cortical feedback in amygdala during behavioral states associated with high cholinergic tone. In this way, ACh would prioritize amygdala inputs to facilitate encoding of emotional memories and attention to novel cues.

References

- Ahmed N, Headley DB, Pare D (2021) Optogenetic study of central medial and paraventricular thalamic projections to the basolateral amygdala. *J Neurophysiol* 126:1234–1247.
- Aitta-aho T, Hay YA, Phillips BU, Saksida LM, Bussey TJ, Paulsen O, Apergis-Schoute J (2018) Basal forebrain and brainstem cholinergic neurons differentially impact amygdala circuits and learning-related behavior. *Curr Biol* 28:2557–2569.e4.
- Amir A, Paré JF, Smith Y, Paré D (2019) Midline thalamic inputs to the amygdala: ultrastructure and synaptic targets. *J Comp Neurol* 527:942–956.
- Arruda-Carvalho M, Clem RL (2014) Pathway-selective adjustment of prefrontal-amygdala transmission during fear encoding. *J Neurosci* 34:15601–15609.
- Baker AL, O'Toole RJ, Gullledge AT (2018) Preferential cholinergic excitation of corticopontine neurons. *J Physiol* 596:1659–1679.
- Baxter MG, Murray EA (2002) The amygdala and reward. *Nat Rev Neurosci* 3:563–573.
- Bell LA, Bell KA, McQuiston AR (2013) Synaptic muscarinic response types in hippocampal CA1 interneurons depend on different levels of presynaptic activity and different muscarinic receptor subtypes. *Neuropharmacology* 73:160–173.
- Bloem B, Poorthuis RB, Mansvelder HD (2014) Cholinergic modulation of the medial prefrontal cortex: the role of nicotinic receptors in attention and regulation of neuronal activity. *Front Neural Circuits* 8:17.
- Bocchio M, Nabavi S, Capogna M (2017) Synaptic plasticity, engrams, and network oscillations in amygdala circuits for storage and retrieval of emotional memories. *Neuron* 94:731–743.
- Cheng Q, Yakel JL (2014) Presynaptic $\alpha 7$ nicotinic acetylcholine receptors enhance hippocampal mossy fiber glutamatergic transmission via PKA activation. *J Neurosci* 34:124–133.
- Chiu CQ, Castillo PE (2008) Input-specific plasticity at excitatory synapses mediated by endocannabinoids in the dentate gyrus. *Neuropharmacology* 54:68–78.
- Christoffel DJ, Walsh JJ, Hoerbelt P, Heifets BD, Llorach P, Lopez RC, Ramakrishnan C, Deisseroth K, Malenka RC (2021) Selective filtering of excitatory inputs to nucleus accumbens by dopamine and serotonin. *Proc Natl Acad Sci USA* 118:e2106648118.
- Christofi FL, Palmer JM, Wood JD (1991) Neuropharmacology of the muscarinic antagonist telazepine in myenteric ganglia of the guinea-pig small intestine. *Eur J Pharmacol* 195:333–339.
- Corcoran KA, Quirk GJ (2007) Activity in prefrontal cortex is necessary for the expression of learned, but not innate, fears. *J Neurosci* 27:840–844.
- Crouse R, Kim K, Batchelor HM, Girardi EM, Kamaletdinova R, Chan J, Rajebhosale P, Pittenger ST, Role LW, Talmage DA, Jing M, Li Y, Gao XB, Mineur YS, Picciotto MR (2020) Acetylcholine is released in the basolateral amygdala in response to predictors of reward and enhances the learning of cue-reward contingency. *Elife* 9:e57335.
- Dannenberg H, Young K, Hasselmo M (2017) Modulation of hippocampal circuits by muscarinic and nicotinic receptors. *Front Neural Circuits* 11:1–18.
- Dasari S, Gullledge AT (2011) M1 and M4 receptors modulate hippocampal pyramidal neurons. *J Neurophysiol* 105:779–792.
- Disney AA, Higley MJ (2020) Diverse spatiotemporal scales of cholinergic signaling in the neocortex. *J Neurosci* 40:720–725.
- Domenici MR, Azad SC, Marsicano G, Schierloh A, Wotjak CT, Dodt HU, Zieglgänsberger W, Lutz B, Rammes G (2006) Cannabinoid receptor type

- 1 located on presynaptic terminals of principal neurons in the forebrain controls glutamatergic synaptic transmission. *J Neurosci* 26:5794–5799.
- Dorje F, Wess J, Lambrecht G, Tacke R, Mutschler E, Brann MR (1991) Antagonist binding profiles of five cloned human muscarinic receptor subtypes. *J Pharmacol Exp Ther* 256:727–733.
- Fitzgerald ML, Mackie K, Pickel VM (2019) Ultrastructural localization of cannabinoid CB1 and mGluR5 receptors in the prefrontal cortex and amygdala. *J Comp Neurol* 527:2730–2741.
- Foster DJ, Wilson JM, Remke DH, Mahmood MS, Uddin MJ, Wess J, Patel S, Marnett LJ, Niswender CM, Jones CK, Xiang Z, Lindsley CW, Rook JM, Conn PJ (2016) Antipsychotic-like effects of M4 positive allosteric modulators are mediated by CB2 receptor-dependent inhibition of dopamine release. *Neuron* 91:1244–1252.
- Gigout S, Wierschke S, Lehmann TN, Horn P, Dehnicke C, Deisz RA (2012) Muscarinic acetylcholine receptor-mediated effects in slices from human epileptogenic cortex. *Neuroscience* 223:399–411.
- Gil Z, Connors BW, Amitai Y (1997) Differential regulation of neocortical synapses by neuromodulators and activity. *Neuron* 19:679–686.
- Giniatullin R, Nistri A, Yakel JL (2005) Desensitization of nicotinic ACh receptors: shaping cholinergic signaling. *Trends Neurosci* 28:371–378.
- Goswamee P, McQuiston AR (2019) Acetylcholine release inhibits distinct excitatory inputs onto hippocampal CA1 pyramidal neurons via different cellular and network mechanisms. *Front Cell Neurosci* 13:1–15.
- Grafe EL, Fontaine CJ, Thomas JD, Christie BR (2021) Effects of prenatal ethanol exposure on choline-induced long-term depression in the hippocampus. *J Neurophysiol* 126:1622–1634.
- Hangya B, Ranade SP, Lorenc M, Kepecs A (2015) Central cholinergic neurons are rapidly recruited by reinforcement feedback. *Cell* 162:1155–1168.
- Hasselmo ME (2006) The role of acetylcholine in learning and memory. *Curr Opin Neurobiol* 16:710–715.
- Hasselmo ME, Sarter M (2011) Modes and models of forebrain cholinergic neuromodulation of cognition. *Neuropsychopharmacology* 36:52–73.
- Hatton GI, Yang QZ (2002) Synaptic potentials mediated by alpha 7 nicotinic acetylcholine receptors in supraoptic nucleus. *J Neurosci* 22:29–37.
- Hedrick T, Danskin B, Larsen RS, Ollerenshaw D, Groblewski P, Valley M, Olsen S, Waters J (2016) Characterization of channelrhodopsin and archaerhodopsin in cholinergic neurons of Cre-Lox transgenic mice. *PLoS One* 11:e0156596.
- Hille B (1994) Modulation of ion-channel function by G-protein-coupled receptors. *Trends Neurosci* 17:531–536.
- Hoffman DA, Johnston D (1998) Downregulation of transient K⁺ channels in dendrites of hippocampal CA1 pyramidal neurons by activation of PKA and PKC. *J Neurosci* 18:3521–3528.
- Howe AR, Surmeier DJ (1995) Muscarinic receptors modulate N-, P-, and L-type Ca²⁺ currents in rat striatal neurons through parallel pathways. *J Neurosci* 15:458–469.
- Janak PH, Tye KM (2015) From circuits to behaviour in the amygdala. *Nature* 517:284–292.
- Jiang L, Kundu S, Lederman JD, López-Hernández GY, Ballinger EC, Wang S, Talmage DA, Role LW (2016) Cholinergic signaling controls conditioned fear behaviors and enhances plasticity of cortical-amygdala circuits. *Neuron* 90:1057–1070.
- Jiang L, Role LW (2008) Facilitation of cortico-amygdala synapses by nicotine: activity-dependent modulation of glutamatergic transmission. *J Neurophysiol* 99:1988–1999.
- Kellis DM, Kaigler KF, Witherspoon E, Fadel JR, Wilson MA (2020) Cholinergic neurotransmission in the basolateral amygdala during cued fear extinction. *Neurobiol Stress* 13:100279.
- Kim J, Isokawa M, Ledent C, Alger BE (2002) Activation of muscarinic acetylcholine receptors enhances the release of endogenous cannabinoids in the hippocampus. *J Neurosci* 22:10182–10191.
- Kodirov S, Jasiewicz J, Amirahani P, Psyrakis D, Bonni K, Wehrmeister M, Lutz B (2009) Endogenous cannabinoids trigger the depolarization-induced suppression of excitation in the lateral amygdala. *Learn Mem* 17:43–49.
- Kurowski P, Gawlak M, Szulczyk P (2015) Muscarinic receptor control of pyramidal neuron membrane potential in the medial prefrontal cortex (mPFC) in rats. *Neuroscience* 303:474–488.
- Lebois EP, Thorn C, Edgerton JR, Popielek M, Xi S (2018) Muscarinic receptor subtype distribution in the central nervous system and relevance to aging and Alzheimer's disease. *Neuropharmacology* 136:362–373.
- LeDoux JE, Cicchetti P, Xagoraris A, Romanski LM (1990) The lateral amygdaloid nucleus: sensory interface of the amygdala in fear conditioning. *J Neurosci* 10:1062–1069.
- Lee MG, Hassani OK, Alonso A, Jones BE (2005) Cholinergic basal forebrain neurons burst with theta during waking and paradoxical sleep. *J Neurosci* 25:4365–4369.
- Li R, Nishijo H, Wang Q, Uwano T, Tamura R, Ohtani O, Ono T (2001) Light and electron microscopic study of cholinergic and noradrenergic elements in the basolateral nucleus of the rat amygdala: evidence for interactions between the two systems. *J Comp Neurol* 439:411–425.
- Liu W, Kumar A, Alreja M (1998) Excitatory effects of muscarine on septo-hippocampal neurons: involvement of M3 receptors. *Brain Res* 805:220–233.
- Marsicano G, Lutz B (1999) Expression of the cannabinoid receptor CB1 in distinct neuronal subpopulations in the adult mouse forebrain. *Eur J Neurosci* 11:4213–4225.
- McGaugh JL (2004) The amygdala modulates the consolidation of memories of emotionally arousing experiences. *Annu Rev Neurosci* 27:1–28.
- Mineur YS, Cahuzac EL, Mose TN, Bentham MP, Plantenga ME, Thompson DC, Picciotto MR (2018) Interaction between noradrenergic and cholinergic signaling in amygdala regulates anxiety- and depression-related behaviors in mice. *Neuropsychopharmacology* 43:2118–2125.
- Mineur YS, Fote GM, Blakeman S, Cahuzac EL, Newbold SA, Picciotto MR (2016) Multiple nicotinic acetylcholine receptor subtypes in the mouse amygdala regulate affective behaviors and response to social stress. *Neuropsychopharmacology* 41:1579–1587.
- Morishita W, Kirov SA, Pitler TA, Martin LA, Lenz RA, Alger BE (1997) N-ethylmaleimide blocks depolarization-induced suppression of inhibition and enhances GABA release in the rat hippocampal slice in vitro. *J Neurosci* 17:941–950.
- Moriya H, Takagi Y, Nakanishi T, Hayashi M, Tani T, Hirotsu I (1999) Affinity profiles of various muscarinic antagonists for cloned human muscarinic acetylcholine receptor (mAChR) subtypes and mAChRs in rat heart and submandibular gland. *Life Sci* 64:2351–2358.
- Muller JF, Mascagni F, McDonald AJ (2011) Cholinergic innervation of pyramidal cells and parvalbumin-immunoreactive interneurons in the rat basolateral amygdala. *J Comp Neurol* 519:790–805.
- Muller JF, Mascagni F, Zaric V, McDonald AJ (2013) Muscarinic cholinergic receptor M1 in the rat basolateral amygdala: ultrastructural localization and synaptic relationships to cholinergic axons. *J Comp Neurol* 521:1743–1759.
- Ohno-Shosaku T, Kano M (2014) Endocannabinoid-mediated retrograde modulation of synaptic transmission. *Curr Opin Neurobiol* 29:1–8.
- Ohno-Shosaku T, Matsui M, Fukudome Y, Shosaku J, Tsubokawa H, Taketo MM, Manabe T, Kano M (2003) Postsynaptic M1 and M3 receptors are responsible for the muscarinic enhancement of retrograde endocannabinoid signalling in the hippocampus. *Eur J Neurosci* 18:109–116.
- Onaivi ES, et al. (2008) Functional expression of brain neuronal CB2 cannabinoid receptors are involved in the effects of drugs of abuse and in depression. *Ann NY Acad Sci* 1139:434–449.
- Palacios-Filardo J, Udakis M, Brown GA, Tehan BG, Congreve MS, Nathan PJ, Brown AJ, Mellor JR (2021) Acetylcholine prioritises direct synaptic inputs from entorhinal cortex to CA1 by differential modulation of feed-forward inhibitory circuits. *Nat Commun* 12:1–16.
- Pancani T, Bolarinwa C, Smith Y, Lindsley CW, Conn PJ, Xiang Z (2014) M4 mAChR-mediated modulation of glutamatergic transmission at corticostriatal synapses. *ACS Chem Neurosci* 5:318–324.
- Perumal MB, Sah P (2022) A protocol to investigate cellular and circuit mechanisms generating sharp wave ripple oscillations in rodent basolateral amygdala using ex vivo slices. *STAR Protoc* 3:101085.
- Power AE, Vazdarjanova A, McGaugh JL (2003) Muscarinic cholinergic influences in memory consolidation. *Neurobiol Learn Mem* 80:178–193.
- Quick MW, Lester RA (2002) Desensitization of neuronal nicotinic receptors. *J Neurobiol* 53:457–478.
- Raiteri M, Marchi M, Costi A, Volpe G (1990) Endogenous aspartate release in the rat hippocampus is inhibited by M2 'cardiac' muscarinic receptors. *Eur J Pharmacol* 177:181–187.
- Salay LD, Ishiko N, Huberman AD (2018) A midline thalamic circuit determines reactions to visual threat. *Nature* 557:183–189.
- Salinas JA, Introini-Collison IB, Dalmaz C, McGaugh JL (1997) Posttraining intraamygdala infusions of oxotremorine and propranolol modulate

- storage of memory for reductions in reward magnitude. *Neurobiol Learn Mem* 68:51–59.
- Sarter M, Lustig C (2020) Forebrain cholinergic signaling: wired and phasic, not tonic, and causing behavior. *J Neurosci* 40:712–719.
- See RE (2005) Neural substrates of cocaine-cue associations that trigger relapse. *Eur J Pharmacol* 526:140–146.
- See RE, McLaughlin J, Fuchs RA (2003) Muscarinic receptor antagonism in the basolateral amygdala blocks acquisition of cocaine-stimulus association in a model of relapse to cocaine-seeking behavior in rats. *Neuroscience* 117:477–483.
- Shapiro MS, Wollmuth LP, Hille B (1994) Modulation of Ca^{2+} channels by PTX-sensitive G-proteins is blocked by N-ethylmaleimide in rat sympathetic neurons. *J Neurosci* 14:7109–7116.
- Sheffler DJ, Williams R, Bridges TM, Xiang Z, Kane AS, Byun NE, Jadhav S, Mock MM, Zheng F, Lewis LM, Jones CK, Niswender CM, Weaver CD, Lindsley CW, Conn PJ (2009) A novel selective muscarinic acetylcholine receptor subtype 1 antagonist reduces seizures without impairing hippocampus-dependent learning. *Mol Pharmacol* 76:356–368.
- Stujenske JM, Likhtik E, Topiwala MA, Gordon JA (2014) Fear and safety engage competing patterns of theta-gamma coupling in the basolateral amygdala. *Neuron* 83:919–933.
- Sugita S, Uchimura N, Jiang ZG, North RA (1991) Distinct muscarinic receptors inhibit release of gamma-aminobutyric acid and excitatory amino acids in mammalian brain. *Proc Natl Acad Sci USA* 88:2608–2611.
- Sun YG, Pita-Almenar JD, Wu CS, Renger JJ, Uebele VN, Lu HC, Beierlein M (2013) Biphasic cholinergic synaptic transmission controls action potential activity in thalamic reticular nucleus neurons. *J Neurosci* 33:2048–2059.
- Suzuki E, Momiyama T (2021) M1 muscarinic acetylcholine receptor-mediated inhibition of GABA release from striatal medium spiny neurons onto cholinergic interneurons. *Eur J Neurosci* 53:796–813.
- Tang B, Luo D, Yang J, Xu XY, Zhu BL, Wang XF, Yan Z, Chen GJ (2015) Modulation of AMPA receptor mediated current by nicotinic acetylcholine receptor in layer I neurons of rat prefrontal cortex. *Sci Rep* 5:14099.
- Unal CT, Pare D, Zaborszky L (2015) Impact of basal forebrain cholinergic inputs on basolateral amygdala neurons. *J Neurosci* 35:853–863.
- Urban-Ciecko J, Jouhanneau JS, Myal SE, Poulet JF, Barth AL (2018) Precisely timed nicotinic activation drives SST inhibition in neocortical circuits. *Neuron* 97:611–625.e5.
- Venkatachalam V, Cohen AE (2014) Imaging GFP-based reporters in neurons with multiwavelength optogenetic control. *Biophys J* 107:1554–1563.
- Venkatesan S, Lambe EK (2020) ChRNA5 is essential for a rapid and protected response to optogenetic release of endogenous acetylcholine in prefrontal cortex. *J Neurosci* 40:7255–7268.
- Watson N, Daniels DV, Ford AP, Eglen RM, Hegde SS (1999) Comparative pharmacology of recombinant human M3 and M5 muscarinic receptors expressed in CHO-K1 cells. *Br J Pharmacol* 127:590–596.
- Wilson MA, Fadel JR (2017) Cholinergic regulation of fear learning and extinction. *J Neurosci Res* 95:836–852.
- Woolf NJ (1991) Cholinergic systems in mammalian brain and spinal cord. *Prog Neurobiol* 37:475–524.
- Xiang Z, Thompson AD, Jones CK, Lindsley CW, Conn PJ (2012) Roles of the M1 muscarinic acetylcholine receptor subtype in the regulation of basal ganglia function and implications for the treatment of Parkinson's disease. *J Pharmacol Exp Ther* 340:595–603.
- Yajeya J, De La Fuente A, Criado JM, Bajo V, Sanchez-Riolobos A, Heredia M (2000) Muscarinic agonist carbachol depresses excitatory synaptic transmission in the rat basolateral amygdala in vitro. *Synapse* 38:151–160.
- Yamada J, Saitow F, Satake S, Kiyohara T, Konishi S (1999) GABA(B) receptor-mediated presynaptic inhibition of glutamatergic and GABAergic transmission in the basolateral amygdala. *Neuropharmacology* 38:1743–1753.
- Yan Z, Surmeier DJ (1996) Muscarinic (m2/m4) receptors reduce N- and P-type Ca^{2+} currents in rat neostriatal cholinergic interneurons through a fast, membrane-delimited, G-protein pathway. *J Neurosci* 16:2592–2604.
- Yang D, Günter R, Qi G, Radnikow G, Feldmeyer D (2020) Muscarinic and nicotinic modulation of neocortical layer 6A synaptic microcircuits is cooperative and cell-specific. *Cereb Cortex* 30:3528–3542.
- Zaborszky L, van den Pol A, Gyengesi E (2012) in *The mouse nervous system, The basal forebrain cholinergic projection system in mice*, eds Watson C, Paxinos G, Puelles L, (Amsterdam, Elsevier), pp 684–718.
- Zhang W, Basile AS, Gomeza J, Volpicelli LA, Levey AI, Wess J (2002) Characterization of central inhibitory muscarinic autoreceptors by the use of muscarinic acetylcholine receptor knock-out mice. *J Neurosci* 22:1709–1717.